

1
2
3
4 **Using machine learning to predict soil bulk density on the basis of visual**
5 **parameters: tools for in-field and post-field evaluation**
6
7

8 **Giulia Bondi^{a*}, Rachel Creamer^b, Alessio Ferrari^c, Owen Fenton^a, David**
9 **Wall^a**
10

11
12 *^aTeagasc Crops, Environment and Land-Use Research Centre, Wexford, Ireland;*

13
14 *^bSoil Biology and Biological Soil Quality, Wageningen University, Wageningen, The*
15 *Netherlands;*

16
17 *^cConsiglio Nazionale delle Ricerche, Istituto di Scienza e Tecnologie dell'Informazione "A.*
18 *Faedo" (CNR-ISTI), Pisa, Italy.*

19
20
21
22
23 ***Corresponding author:** G. Bondi (Email: Giulia.Bondi@teagasc.ie)

24
25 R. Creamer (Email: rachel.creamer@wur.nl); A. Ferrari (Email: alessio.ferrari@isti.cnr.it);

26
27 O. Fenton (Email: Owen.Fenton@teagasc.ie); D. Wall (Email: David.Wall@teagasc.ie).
28
29
30
31

32 **Abstract**
33

34 Soil structure is a key factor that supports all soil functions. Extracting intact
35 soil cores and horizon specific samples for determination of soil physical
36 parameters (e.g. bulk density (B_d) or particle size distribution) is a common
37 practice for assessing indicators of soil structure. However, these are often
38 difficult to measure, since they require expensive and time consuming
39 laboratory analyses. Our aim was to provide tools, through the use of machine
40 learning techniques, to estimate the value of B_d based solely on soil visual
41 assessment, observed by operators directly in the field. The first tool was a
42 decision tree model, derived through a decision tree learning algorithm, which
43 allows discrimination amongst three B_d ranges. The second tool was a linear
44 equation model, derived through a linear regression algorithm, which predicts
45 the numerical value of soil B_d . These tools were validated on a dataset of 471
46
47
48
49
50
51
52
53
54
55
56
57
58
59

60
61
62 soil horizons, belonging to 201 soil profile pits surveyed in Ireland. Overall, the
63 decision tree model showed an accuracy of ~60%, while the linear equation
64 model has a correlation coefficient of about 0.65 compared to the measured B_d
65 values. For both models, the most relevant property affecting soil structural
66 quality appears to be the humic characteristics of the soil, followed by soil
67 porosity and pedogenic formation. The two tools are parsimonious and can be
68 used by soil surveyors and analysts who need to have an approximate in-situ
69 estimate of the structural quality for various soil functional applications.
70
71
72
73
74
75
76
77
78
79
80

81 **Keywords:** soil bulk density, soil structure, soil quality, machine learning
82
83
84
85

86 **1. Introduction**

87

88 The importance of soil structure in relation to soil quality is well known
89 (Mueller et al., 2009; Karlen, 2004; Kay et al., 2006). A commonly used soil
90 physical measurement to characterize soil structural quality is soil bulk density
91 (B_d) (Armino and Wendroth, 2016; Dam et al., 2005; Håkansson and Lipiec,
92 2000; Logsdon and Karlen, 2004; Moncada et al., 2015), which is defined as the
93 oven-dry mass per unit volume of soil (IUSS Working Group, 2006; Mueller et
94 al., 2009). Measurement of soil B_d is useful as it describes both the packing
95 structure of the soil and its permeability (Dexter, 1988), whereby drainage
96 characteristics can be inferred (Reidy et al., 2016). B_d measurement is often
97 used in agronomic studies as it indicates the presence of compacted layers
98 resulting from machinery or animal traffic (Reidy et al., 2016; Saffih-Hdadi,
99 2009), which may affect crop production. It is commonly considered an
100 efficient measurement of soil carbon and nutrient stocks (Ellert and Bettany,
101 1995; Reidy et al., 2016).
102
103
104
105
106
107
108
109
110
111
112
113
114
115
116
117
118

119
120
121
122 However, the process of measuring B_d is often time consuming and open to
123 human bias in the field and requires accurate laboratory analyses using trained
124 personnel. Furthermore, soil texture has an important influence on the
125 assessment of B_d e.g. in soils with high clay or sand content, or very humic
126 soils, it may be difficult to obtain a representative sample and large variability
127 between replicate samples can represent a problem. Also, in some soils the
128 presence of stones can make sampling almost unmanageable. For such reasons,
129 or constraints of budget or laboratory facilities, B_d measurements are commonly
130 missing from soil databases (Reidy et al., 2016).
131
132
133
134
135
136
137
138

139 The main methods employed for the prediction of B_d are pedotransfer functions
140 (PTF) methods, based on measurable soil attributes, such as organic carbon
141 (OC) and clay content (Kaur et al., 2002; Leonavičiūtė, 2000; Reidy et al.,
142 2016). However, many of these methods ignore horizonation and depth
143 variances for soil B_d prediction (Reidy et al., 2016). Furthermore, the nature of
144 these methods, based on chemical/physical or landscape parameters, do not
145 capture the intrinsic nature of the soil structural properties.
146
147
148
149
150
151
152

153 Our experience with respect to soil descriptions and classification has shown
154 that the visual observations collected in the field at horizon level are often very
155 important for the evaluation of soil quality (Fenton et al., 2017; 2015) and they
156 become essential during the interpretation of the trend of some analytical
157 parameters used as indicators of soil structure status e.g. B_d .
158
159
160
161

162 Soil structural quality has been assessed visually for millennia (Batey, 2000)
163 e.g. soil survey manuals used in the field such as the Soils Survey Division Staff
164 Manual (1993) or the WRB for soil resources (FAO, ISRIC and ISSS, 1998)
165 include soil structure visual observations. However, soil scientists, for a long
166 time, have presented repeatable procedures for the examination of soil structural
167
168
169
170
171
172
173
174
175
176
177

178
179
180 form, stability and resilience (see latest review by Emmet-Booth et al., 2016
181 with examples from 1940's to present; Ball and Munkholm, 2015).
182
183
184

185 Taking this into account, in the present work we investigated whether, and to
186 what extent those visual observations, called descriptors, can be used to predict
187 soil B_d , which is considered one of the most efficient indicators in the
188 assessment of soil structure quality (Moncada et al., 2015).
189
190
191

192
193 In order to achieve this objective, machine learning techniques were used. The
194 potential of machine learning techniques have been rediscovered in the last few
195 years through various applications in environmental sciences.
196
197
198

199 Worldwide, decision tree approaches have been used for different purposes:
200 identifying sources of soil pollution (Xue et al., 2015); describing the extension
201 of different forms of soil erosion in Mexico (Geissen et al., 2007); predicting
202 chemical soil properties at national level in Australia (Henderson et al., 2005);
203 classifying the surface soil freeze/thaw status in China (Jin et al., 2009) and
204 even studying of soil structure through the prediction of soil hydraulic
205 properties (Pachepsky and Rawls, 2003). However, limited literature has been
206 found on the use of these powerful tools for environmental science in Europe.
207
208
209
210
211
212
213
214

215 The decision tree model output applied in this paper is based on a series of rules
216 generated by the software, which can be visualised as paths starting from the
217 root of the decision tree and ending at one of the leaves (Bhargava et al., 2013;
218 Xue et al., 2013; Xue et al., 2015). Each of those paths corresponds to one or
219 more soil *descriptors*, which are related to an internal *node* (Henderson et al.,
220 2005). The model is able to examine all possible descriptors and then to select
221 the most decisive *splitting attribute* (Xue et al., 2013). This operation occurs
222 several times until all the instances are correctly classified in a set of *rules*. Each
223 descriptor included in the model corresponds to a more defined *level* of
224 classification.
225
226
227
228
229
230
231
232
233
234
235
236

237
238
239 The linear regression model applied in this paper is a classical statistical
240 technique used to predict numerical data. It is based on the modelling of the
241 relationship between a scalar dependent variable and one or more explanatory
242 variables.
243
244
245
246
247

248
249 With our work we want to:

250
251 (i) Provide an operational strategy to estimate a range of B_d values, based on the
252 visual soil parameters by means of a decision tree approach. This model can be
253 used as a field tool to predict a general class of B_d (Low, Medium and High). It
254 is an instrument able to discriminate between macro classes and has to be
255 considered as a descriptive tool for *qualitative* estimation.
256
257
258
259

260
261 (ii) Propose an algorithm that can predict a numerical estimate of B_d . This
262 second model should discriminate better between smaller increments. This
263 instrument has to be considered as a more refined tool for *quantitative*
264 estimation.
265
266
267
268
269

270 **2. Methods**

271 **2.1 Primary data source and descriptors**

272
273 Two pedological surveys, where full soil profile descriptions and supporting
274 laboratory analyses, were carried out in Ireland with the aim of defining a
275 coherent and homogeneous way to study soil formation, functions and quality:
276
277
278

- 279
280 1. The Irish Soil Information System (Irish SIS) project was established in
281 2008. It aimed to conduct a programme of structured research into the
282 national distribution of soil types and construct a soil map, at 1:250,000
283 scale, able to identify and describe the soils according to a harmonised
284 national legend. Irish SIS included more than 225 sites distributed around
285 Ireland (Creamer et al., 2014).
286
287
288
289
290
291
292
293
294
295

- 296
297
298
299
300
301
302
303
304
305
306
307
308
309
2. The Soil Quality and Research project (SQUARE) started in 2013. The aim was to establish a baseline of soil quality in Ireland. The SQUARE soil survey included 38 grassland sites distributed within the five major agro climatic regions of Ireland defined by Holden and Bereton (2004) and classified into two drainage classes on the basis of the Irish Soil classification System.

310
311
312
313
314
315
316
317
318
319

During both (1) and (2) profile pits approximately 1 m deep, were observed and described by different operators. For the present study data from 201 profiles (168 Irish SIS, 33 SQUARE) was extracted from the larger database to cover a wide variety of Irish soil types with a specific focus on mineral soils. This data represents 471 horizons (<http://gis.teagasc.ie/soils/map.php>).

320
321
322
323
324
325
326
327
328
329
330
331
332
333
334
335
336
337
338
339
340
341
342
343

Although different surveyors worked across the projects mentioned, a systematic procedure was applied to describe the nature of the soil profiles, which included each of the soil horizons. Training was given to field operators. Using knowledge of soil structure and quality, the operators followed a widely understood schema of observation (developed by FAO through the Guidelines for Soil Description in 2006) which was able to investigate and finally characterize soil structure through visual parameters (FAO, 2006; FAO, ISRIC and ISS, 1998). Herein we have selected eleven descriptors presented in Table 1 (justifications are provided in Table 1), which may be considered the most important for the qualitative judgment of soil structure. Each descriptor was described and recorded on the basis of a set of pre-defined categories, reported in Table 1 in the Supplementary Material.

344 345 346

2.2 Soil analysis

347
348
349
350
351
352
353
354

The procedure to determine B_d of intact cores is a version of the ISO 11272:1998 – Soil Quality Part 5: Physical methods Sect. 5.6 – Determination of dry bulk density. The primary difference between the ISO and the applied

355
356
357 methodology is that the ISO does not account for stone mass and volume in its
358 core method, whereas the methodology applied in this study includes the
359 following equation to calculate B_d (stone free):
360
361
362
363

$$364 \quad B_d \text{ (g cm}^{-3}\text{)} = (Md - Ms)/(V - Vs) \quad \text{Eq 1}$$

365
366
367 where; Md: oven dry soil material weight (g), Ms: oven dry stone weight (g), V:
368 volume of soil core (cm^{-3}), Vs: volume of stones (mL). Soil B_d values reported
369 in this paper correspond to the mean of the three values obtained for each
370 horizon sampled.
371
372
373
374
375
376
377

378 **2.3 Model frameworks**

379 Two models were built by means of the modelling tool WEKA (Waikato
380 Environment for Knowledge Analysis). WEKA 3.8 is open source software for
381 machine learning and data mining under the General public license developed at
382 the University of Waikato in New Zealand
383 (<http://www.cs.waikato.ac.nz/ml/weka>, Bhargava et al., 2013). This software
384 includes different implementations of several machine learning algorithms. In
385 our context, we used two specific algorithms that are made available by the tool,
386 namely:
387
388
389
390
391
392
393

- 394 • the j48 algorithm, which corresponds to the WEKA's implementation of the
395 C4.5 decision tree learner (Quinlan, 1993; Xue et al., 2015) which was used
396 to build Model (1);
397
398
- 399 • a linear regression algorithm, used to build the Model (2). The M5 Method
400 was used as attribute selection method for the linear model presented.
401
402
403
404

405
406 Two models were produced to achieve the objectives of our work:
407
408
409
410
411
412
413

- 414
415
416
417
418
419
420
421
422
423
424
425
426
427
- Model (1) is based on a classic decision tree model, developed to be used in the field in order to predict a B_d class using only visual descriptors as in Table 1.
 - Model (2) is a linear regression model that uses the same in-field descriptors as above, and it is able to predict a numerical value of B_d with a relatively small error.

428
429
430
431
432
433
434
435
436
437
438
439
440

The proposed two models are both descriptive and predictive, but the decision tree is better at exploring in a descriptive way the relationship between B_d and visual parameters, as it allows further analysis of the soil pertaining to that soils own chemical and physical characteristics. On the other hand, the linear equation algorithm is stronger as a predictive tool and it offers a more precise estimate of B_d .

441 **2.3.1 Data treatment**

442
443
444
445
446
447

The entire database consists in 201 sampling points (profile pits) for a total of 471 horizons. For each horizon eleven descriptors and B_d data were used to train Model (1) and Model (2). The treatment of data can be summarized as follows:

- 448
449
450
451
452
453
454
455
456
457
458
459
460
461
462
463
464
465
466
467
468
469
470
471
472
- Data cleaning: to produce a full dataset, time was invested to ensure the data homogeneity between Irish SIS (649 horizons) and SQUARE datasets (125 horizons). In particular, descriptor rating options were double checked to reaffirm consistency across projects. To achieve uniformity within the dataset some data conversions were necessary. The final dataset consisted of 471 horizons i.e. 346 from Irish SIS and 125 from SQUARE.
 - Missing values imputation: an initial analysis of the dataset highlighted the presence of some missing values for part of the considered descriptors, namely: “Fissure size”, “Void size”, “Void abundance” and “Soil consistency”. To avoid further reductions of the dataset, an IMRI imputation (performed by the WEKA 3.8 software described above) was selected as the means to predict missing values (Templ et al., 2011).

2.3.2 Model 1: Decision tree model, validation and outputs

Model (1) has been designed to predict classes of B_d data through the combination of the 11 visual descriptors outlined in Table 1. The model has been trained using B_d data at horizon level. The predicted classes of B_d are:

- (i) Low B_d class: $< 1.0 \text{ g cm}^{-3}$ (n=137 cases)
- (ii) Medium B_d class: between 1.0 and 1.4 g cm^{-3} (n=178 cases)
- (iii) High B_d class: $> 1.4 \text{ g cm}^{-3}$ (n=156 cases)

Class ranges were selected on the basis of their homogeneity in terms of class population. The B_d measured in the majority of mineral soils under agricultural management in Ireland occur typically within the 1.0 and 1.4 g cm^{-3} range. Values of $< 1.0 \text{ g cm}^{-3}$ are usually related to Ombrotrophic or Mineratrophic Peat Soils (which correlates with the Histosol reference soil group of the WRB (IUSS Working Group WRB, 2006) or mineral soils having a Histic horizon (Reidy et al., 2016). Therefore 1.0 g cm^{-3} was selected as the lower B_d threshold e.g. herein 16 cases out of 137 belonged to the Low B_d class as Oh, Op, Of or Omf. The higher threshold (1.4 g cm^{-3}) was empirically chosen to best fit these data. In particular, multiple decision tree models were trained by varying the threshold between 1.1 g cm^{-3} and 1.8 g cm^{-3} , in 0.1 intervals. The model trained with the 1.4 g cm^{-3} threshold outperformed, other model runs in terms of accuracy.

The decision tree produced herein can be easily converted into classification rules. Each path in the tree that goes from the root to one of the leaves defines one classification rule. In our case each rule categorises the data in B_d Low, Medium and High classes. The knowledge represented in a decision tree can be extracted and represented in the form of the classification rule IF-THEN as follows:

532
533
534 **If** {condition A} AND {condition B} AND {condition C} AND {...} **then**
535 categorization.
536
537
538

539
540 In our case:

541
542 **If**

543 the horizon is described as HUMOSE

544
545
546 **then**

547 the horizon fits into the bulk density category “Low”= $<1 \text{ g cm}^{-3}$
548
549
550

551 A pruning technique is automatically performed by the WEKA software. This
552 allows the identification and the removal of the outliers reducing the risk of
553 overfitting to the training data (Bhargava et al., 2013). When decision trees are
554 built, many of the ramifications can represent noise or outliers in the training
555 data. The pruning process tries to identify and remove these branches with the
556 aim of improving the accuracy of classification of future data. The next step was
557 to prune the dataset to identify and remove branches which do not improve
558 prediction with the aim of improving the accuracy of classification of future
559 data. The pruning process tries to identify and remove these branches with the
560 aim of improving the accuracy of classification of future data. The next step was
561 to prune the dataset to identify and remove branches which do not improve
562 prediction with the aim of improving the accuracy of classification of future
563 data. The pruning process tries to identify and remove these branches with the
564 aim of improving the accuracy of classification of future data. The next step was
565 to prune the dataset to identify and remove branches which do not improve
566 prediction with the aim of improving the accuracy of classification of future
567 data.
568

569 A10-fold cross validation method was adopted, which randomly partitions the
570 dataset into 10 parts and is used to validate the model. Then nine parts of the
571 dataset were used to train the model, with the last part used for model testing
572 (see Xue et al., 2015 for a similar approach).
573
574
575
576
577

578
579 Two measures were applied to evaluate the model performance; precision and
580 recall values were calculated. Precision indicates how many of the instances
581 were classified within a certain class that actually belong to that class. Whereas
582 recall indicates how many of the instances that belong to a certain class are
583
584
585
586
587
588
589
590

591
592
593
594 correctly classified by the model. To explain these measures further, it is useful
595 to introduce the concepts of true positive, false positive and false negative.

597 Given a class C , we define true positives tp as the number of instances labelled
598 as C in the original dataset, and classified as C by the decision tree; false
599 positives fp as the number of instances not labelled as C in the original dataset,
600 and incorrectly classified as C by the decision tree; false negatives fn as the
601 number of instances labelled as C in the original dataset, and not classified as C
602 by the decision tree. Given these definitions, precision p_C and recall r_C for the
603 class C are defined as follows:
604
605
606
607
608
609

$$610 \quad p_C = \frac{tp}{tp + fp}; \quad \text{Eq 2}$$

$$611 \quad r_C = \frac{tp}{tp + fn} \quad \text{Eq 3}$$

612
613
614
615
616 Precision is negatively influenced by the number of false positive cases.
617 Whereas, recall is negatively influenced by the number of false negative cases.
618 High scores for precision and recall show that the classifier is returning accurate
619 results (high precision, related to low false positive rates), as well as returning a
620 majority of all positive results (high recall, related to a low false negative rates).
621
622
623
624
625
626

627
628 As no baseline algorithms were available, or proposed in other publications,
629 against which to evaluate the performance of our Model (1), we resort to
630 comparing it with a random predictor baseline, i.e. a fictional algorithm that
631 randomly predicts the class of an instance (Alvarez, 2002).
632
633
634

635 Let n be the total number of instances, and let c be the number of instances of
636 class C , the precision and recall of a random predictor for the class C is given
637 by:
638
639

$$640 \quad p_C = r_C = c / n \quad \text{Eq 4}$$

Besides precision and recall for each class, we also evaluated the average value of these measures. In addition, we evaluated the harmonic means of precision and recall, which is normally called F-measure, and is defined as follows:

$$F\text{-measure} = 2 * \frac{p_c * r_c}{p_c + r_c} \quad \text{Eq 5}$$

Finally, as an overall indicator of the ability of the decision tree to correctly classify the instances, we evaluated the overall accuracy, which is defined as follows:

$$Accuracy (\%) = \frac{tp + tn}{tp + tn + fp + fn} \quad \text{Eq 6}$$

2.3.3 Model 2: Linear regression model, validation and outputs

Using data from the visual parameters (Table 1), a linear equation that predicted an exact B_d value was developed.

As for Model (1), Model (2) was learned using B_d data at horizon level and produced by means of the WEKA software, using a linear regression algorithm. For this experiment these data were converted into numerical binary data, since the linear regression algorithm takes numerical data as input. In particular, for each value taken by each descriptor, a binary variable was created that takes either 0 (False) or 1 (True) as values. The variable was 1 if the descriptor had the value associated to the variable, and 0 otherwise.

The model builds a linear equation based on a weighted combination of the possible values taken by the 11 descriptors. In particular, the linear model has the following form:

$$B_d (g\ cm^{-3}) = \sum_{i=0}^n C_i * V_i \quad \text{Eq 7}$$

where C_i are the coefficients computed by the linear regression algorithm. V_i are the binary variables. The linear regression algorithm is designed to select only those variables that have an influence on the final B_d value. Hence, the final model will not include all the possible variables, but only a subset. A 10-fold cross validation was performed to validate the model as described in par 2.3.2.

For Model (2) we could not evaluate the performance through precision and recall, since numerical values are involved instead of categorical ones, but we evaluated it in terms of correlation coefficient, root mean squared error, and mean absolute error:

The Root Mean Squared Error (RMSE) gives an estimation of the standard deviation of the error (Henderson et al., 2005). The lower is RMSE the higher is the predictive ability. Where n is the size of the dataset and \hat{y}_t is the predicted value, the formula is defined as follows:

$$RMSE = \sqrt{\frac{1}{n} \sum_{t=1}^n (y_t - \hat{y}_t)^2} \quad \text{Eq 8}$$

The Mean Absolute Error (MAE) is a quantity used to measure how close predictions are to the eventual outcomes. The mean absolute error is also known as the mean absolute deviation (Henderson et al., 2005). The lower the MAE value the higher is the predictive ability.

$$MAE = \frac{1}{n} \sum_{t=1}^n |y_t - \hat{y}_t| \quad \text{Eq 9}$$

3. Results and discussion

3.1 Model 1: Decision tree approach to assess B_d classes

3.1.1 Model performances

The number of rules generated by the decision tree algorithm was 41 in total; 11, 13 and 17 for Low, Medium and High respectively (all the rules are reported in Table 2 in the Supplementary Material). ~~The overall tree is reported in was unpacked into three sub-trees, one for each B_d class, to increase output readability (Figure 1s-1-3).~~ The decision tree hierarchy consists of six levels (level 1 has the highest classification power) of depth as follows:

Level (1): Humose

Level (2): Structure type

Level (3): Macropores Size/Void Size/Void Abundance/Plasticity

Level (4): Structure Grade/Stickiness

Level (5): Fissures

Level (6): Structure size

The descriptor “soil consistency” was excluded by the tree hierarchy, showing no influence on the prediction of B_d ranges. To discuss these results, it is useful to associate the different levels and hence, the corresponding descriptors, to specific soil quality properties. Broadly the descriptors that remained in the analysis fell into 4 main groups in order of importance as follows:

(i) soil humic characteristics; explained by level (1);

(ii) pedogenic formation; explained by level (2);

(iii) soil porosity; explained by level (3);

(iv) soil cohesive properties; explained by level (3-4).

The majority of the 41 rules were classified within the first three hierarchical levels highlighting the importance of these soil structural descriptors in quantifying B_d class. In general the parallelism between soil aggregation mechanisms, soil intrinsic characteristics related to soil forming factors, and the

827
828
829 arrangement of solid and voids with their capacity to retain and transmit fluids,
830
831 resulted in the main factors being capable of explaining soil B_d .
832
833
834

835 The overall accuracy shows that the model correctly classified 71% of the
836 training data (Table 2). However, after the 10-fold cross validation step the
837 model was able to correctly predict 60% of the cases (Table 2). The confusion
838 matrix shows that mis-categorisation does not occur from Low to High B_d
839 classes and vice versa, but can occur from Low to Medium (46 cases) and from
840 High to medium (52 cases) (Table 3). The cause of lower model performance
841 can be clarified by looking at the branches of the decision tree that miss-classify
842 the highest number of instances (for discussion see par. 3.2.1).
843
844
845
846
847
848
849
850

851 The decision tree model was evaluated using the random predictor method (see
852 par. 2.3.2). Performances are the following:
853
854

855 Low: $p_L = r_L = 137/471 = 0.29$.

856 Medium: $p_M = r_M = 178/471 = 0.37$.

857 High: $p_H = r_H = 156/471 = 0.33$.
858
859
860
861
862

863 For the Low B_d class, the decision tree outperforms a random predictor by 40%
864 in terms of precision and by 25% in terms of recall; for the Medium B_d class, by
865 16% in terms of precision and by 26% in terms of recall; for the High B_d class
866 by 30% in terms of precision and by 29% in terms of recall. These figures
867 indicate that, although the accuracy indicates poor performance for the Low B_d
868 class, the prediction for this class in terms of precision is actually the best
869 amongst all 3 classes. This is due to the lower number of Low B_d instances,
870 which are harder to detect for a random classifier, and that our algorithm
871 predicts with a substantially higher degree of precision. Overall, the
872 classification produced by the model is considerably better than a random
873 classification.
874
875
876
877
878
879
880
881
882
883
884
885

3.1.2 Rules analysis

Figures 1-3 show the decision tree generated for each B_d class with the corresponding instances classified for each rule and the percentage of accuracy, which refers to the percentage of true positive cases found by the model for the rule discussed. Rules classifying less than two instances are not reported in these figures.

- **Level 1: “Humose”**

The “**Humose**” descriptor emerges as the most dominant discriminator. All the horizons that highlight the presence of the “humose” feature following the rule “Humose: *yes*”, fit in the category Low B_d . The model correctly classifies 85.9% of $n=64$ instances for this rule with relatively few false positive cases.

The humose feature refers to an estimation of the level of humification of the organic material, so it is indirectly related to the C content. In fact, soil OC content gives an indication of decomposition rates which have a direct effect on soil aggregation (Bronick and Lal, 2005; Schulten and Leinweber, 2000). The presence of humic substances, as well decomposed organic matter (OM), contributes to the stability of soil aggregates and pores through the bonding or adhesion properties of organic materials, such as bacterial waste products, organic gels, fungal hyphae and worm secretions and casts. Moreover, OM intimately mixed with mineral soil materials induces increased moisture holding capacity and air exchange with the atmosphere (Stevenson, 1994). This mechanism is reflected by lower values of B_d , resulting in enhancement of soil porosity producing a good soil structure.

When the humose feature is recorded as absent, the model switches to level 2 for further refinement.

945
946
947
948
949
950
951
952
953
954
955
956

- **Level 2: “Structure Type”: Granular**

957
958
959
960
961
962
963
964
965
966
967
968
969
970
971
972
973
974
975
976
977
978
979
980
981
982

“Structure Type” was the most discriminating descriptor at the second level of the tree hierarchy. Here the tree branches out to account for the effect of different types of structure.

983
984
985
986
987
988
989
990
991
992
993
994
995
996
997
998
999
1000
1001
1002
1003

For the rule “Humose: *no*, AND Structure type: *Granular*” the model classified 23 cases as belonging to the Low B_d class, with an accuracy of 56.5%. Despite the high number of false positives, the amplitude of the group is among the highest, showing its reliability.

Granular aggregates are spheroids or polyhedrons aggregates of soil, having curved or irregular surfaces (FAO, 2006), they are normally associated with highest air capacity, and are an indicator of good soil structure (Mueller et al., 2009). Such cases are mostly A horizons, not deeper than 30 cm. Root mass, density, distribution and turnover, can positively influence the soil particle aggregation by releasing a variety of compounds, (such as root exudates) and can contribute to increased soil porosity through mechanical action (Bronick and Lal, 2005; Caravaca et al., 2002). This is reflected in the B_d, resulting in lower values.

- **Level 2: “Structure Type”: Subangular Blocky → Level 3, “Macropores Size” → Level 4 “Structure Grade”**

In presence of the “Subangular Blocky” structure type the tree branches split again, going deeper into the third hierarchical level of tree structure, showing the “Macropores size” descriptor as the next level of description. For the rules “Humose: *no*, AND Structure type: *Subangular Blocky* AND Macropores: (*A*), (*B*), (*C*), (*D*)”:

(*A*) Coarse (C 5.0-20.0 mm): 50% accuracy when classifying Low B_d class.

(*B*) Fine (F 0.5-2.0 mm): for subangular blocky aggregates, 66.1% accuracy when classifying Medium B_d class. This is a rule that has a higher number of

1004
1005
1006 instances (n=92), which balances the presence of a relatively high number of
1007 false positives. For angular blocky aggregates, 72.7% accuracy when classifying
1008 Medium B_d class (n=11).
1009

1010 (C) Very Fine (VF < 0.5 mm): 66.7% accuracy when classifying High B_d class.
1011

1012 (D) Medium (M 2.0-5.0 mm): 100% accuracy when classifying Low and
1013 Medium B_d class.
1014
1015

1016 Subangular blocky structure type is described as cube like with a flat surface
1017 and rounded corners (FAO, 2006; Schoeneberger et al., 2012) and is considered
1018 an indicator of an intermediate degree of soils structure quality, between the
1019 granular/crumby aggregates and the blocky/sharp angular ones. Results for this
1020 structure type show that the size of the macropores is a crucial variable to
1021 discriminate in terms of B_d classes, as B_d is very sensitive to both alteration of
1022 macroporosity abundance and size of pores (Mueller et al., 2009). In particular
1023 the higher the macropore size, the lower the B_d class predicted by the model.
1024
1025
1026
1027
1028
1029
1030
1031
1032
1033

1034 For the rule (A), horizons fitting the Low B_d class are mostly Ap horizons,
1035 corresponding to the upper soil layers (maximum depth of 22 cm). Earthworm
1036 activity is mainly concentrated in the top soil (Haynes and Naidu, 1998; Lee and
1037 Foster, 1991), which promotes macropores (C 5.0-20.0 mm) which in turn can
1038 alter soil porosity thereby affecting the movement of air, water and solutes
1039 (Shipitalo and Le Bayon, 2004). For the rule (B) and (C) medium and high B_d
1040 are associated with macropore sizes from 0.5 mm to 2.0 mm. The cases
1041 following these two rules are mainly classified as A or B horizons for the
1042 medium B_d class (average maximum depth of ~40 cm) and as B horizons for the
1043 higher B_d class (average maximum depth of ~60 cm). At such depths roots
1044 become thinner resulting in reduced porosity and higher B_d. Furthermore, B_d
1045 often increases exponentially in the deeper horizons due to compaction resulting
1046 from an increase in clay material or as result of management operations.
1047
1048
1049
1050
1051
1052
1053
1054
1055
1056
1057
1058
1059
1060
1061
1062

1063
1064
1065
1066
1067
1068
1069
1070
1071
1072
1073
1074
The medium class of macropores (M 2.0-5.0 mm) insufficiently defines the B_d range and must be assisted by another splitting attribute which is triggered at level four. The “**Structure grade**” is identified by the model as an important variable to discriminate between the Low and Medium B_d class for this macropores size. The rule (*D*) is consequently developed as follows:

- 1075 • “Humose: *no*, AND Structure type: *Subangular Blocky* AND Macropores: *M*
1076 *2.0-5.0 mm* AND Structure grade: *Moderate*”; which predict Low B_d class
1077 (100% correct instances).
1078
- 1080 • “Humose: *no*, AND Structure type: *Subangular Blocky* AND Macropores:
1081 *M 2.0-5.0 mm* AND Structure grade: *Weak*”; which predict Medium B_d class
1082 (100% correct instances).
1083
1084
1085

1086
1087
1088
1089
1090
1091
1092
1093
1094
1095
1096
1097
1098
1099
1100
1101
1102
1103
1104
1105
1106
1107
1108
1109
1110
1111
1112
1113
1114
1115
1116
1117
1118
1119
1120
1121
FAO (2006) defines soils by describing the lack (apedal) or the presence (pedal) of a defined structure. A moderate structure grade, showing the presence of a nicely structured soil, was associated with a Low B_d class. Medium B_d classes are associated with a weak structure grade, synonymous of a lower structure quality. However, herein cases classified for these two rules were similar in terms of actual B_d values. In particular, cases classified as Low B_d had actual values very close to the upper limit of this category (values between 0.9 and 1.0 g cm⁻³) and the cases classified as Medium B_d had actual values close to the lower limit of this category (values between 1.0 and 1.16 g cm⁻³). Considering the narrow range of values for these cases across the Low and Medium B_d categories the model correctly discriminates between categories.

- **Level 2: “Structure Type”: Angular Blocky → Level 3, “Void Size” → Level 4 ”Stickiness”**

The “Angular Blocky” aggregates belong to the blocky category as for the subangular blocky aggregates, but differ as they have faces intersecting at relatively sharp angles (FAO, 2006; Schoeneberger et al., 2012). In the presence of this structure type i.e. a typical indicator of a poorly structured soil, the

1122
1123
1124 model returns “**Void size**” as the next, most important, descriptor. This
1125 descriptor indicates the total volume of pores discernible with a *10 hand-lens
1126 (FAO, 2006). It differs from macroporosity as it is a much wider term that
1127 includes soil fissures and plane (FAO, 2006). Macropores are mostly
1128 determined by plant roots through the twisting activity within and around
1129 aggregates, and by zoological exploration, through burrowing activity, so they
1130 are usually larger pores having a size higher than 75 µm (Russell, 1975).
1131 However, here macropores and voids are described in terms of size, so a high
1132 void size can correspond to a high macropores size. Therefore, it is important to
1133 highlight here that although different from a semantic point of view, the
1134 combination of these two descriptors was very effective in explaining soil
1135 porosity.
1136
1137
1138
1139
1140
1141
1142
1143
1144
1145
1146
1147

1148 For the rule “Humose: *no*, AND Structure type: *Angular Blocky* AND Void
1149 size: *C 5.0-20.0 mm*” the model returned 75% of correct instances for the class
1150 Low B_d. Although the structure type indicated was often that of a very poor
1151 structured soil, characterised by large, angular and sharp aggregates, this effect
1152 was mitigated by the presence of a very high overall porosity, resulting in a
1153 Low B_d (Pagliai and Vignozzi, 2002).
1154
1155
1156
1157
1158
1159

1160 The rule “Humose: *no*, AND Structure type: *Angular Blocky* AND Void size:
1161 *VF < 0.5 mm*”, returned High B_d class with 76.9 % accuracy. Also this rule was
1162 quite wide in terms of population (n=26). In this case the poorly structured
1163 horizons were associated with the smallest size of pores. The cases are mainly
1164 classified as B_g, BC_g, C_g or E_g horizons, with an average depth ranging from
1165 42 to 72 cm. For such cases, gleying is caused by surface water which has been
1166 held in a poorly permeable horizon, (mainly belonging to surface water gley soil
1167 type (Stagnosols reference soil group of the WRB). These poorly permeable
1168 layers showed evidence of compaction due to one or more of the following
1169 characteristics: (i) presence of a pan, resulting in severe compaction imposed by
1170
1171
1172
1173
1174
1175
1176
1177
1178
1179
1180

1181
1182
1183 management, (ii) poor structural development, (iii) very heavy textured
1184 horizons dominated by silt and clay and (iv) natural impeded horizons due to
1185 soil formation and profile development mechanisms.
1186
1187

1188
1189 Furthermore, the presence of some argillic horizons classified as Btg following
1190 this rule, as well as having gleyic features, showed the presence of clay-sized
1191 material in coatings or as intrapedal concentrations (FAO, 2006). Clay content
1192 physically affects particle aggregation through swelling and dispersion,
1193 resulting in contiguous peds which fit together eliminating space (Attou et al.,
1194 1998; Bronick et Lal, 2005; Kay, 1998; Russel, 1975).
1195
1196
1197
1198
1199
1200
1201

1202 When the void size is classified as belonging to the middle category (Humose:
1203 *no*, AND Structure type: *Angular Blocky* AND Void size: *F 0.5-2.0 mm*),
1204 “**Stickiness**” was selected by the model as the next most informative descriptor,
1205 associating Medium B_d class with the “*Non Sticky OR Slightly Sticky*” feature
1206 (50% and 63.6% accuracy, respectively), and the High B_d class with the
1207 “*Sticky*” feature (accuracy of 75%). The rules’ population size was n=44, n=22
1208 and n=12, respectively and therefore must be considered an important branch of
1209 the overall tree. As the stickiness property is considered an indirect indicator of
1210 the clay content in soil, the results confirmed that the presence of clay material
1211 was one of the characteristics which makes the soil prone to compaction, or at
1212 least significantly decreases the level of porosity. Even in the presence of a
1213 relatively higher porosity, clay content was crucial to force a split in B_d classes,
1214 thereby attributing higher B_d values to heavier textured soils.
1215
1216
1217
1218
1219
1220
1221
1222
1223
1224
1225
1226
1227

1228 “**Plasticity**” appears at the third depth level of the decision tree for the
1229 structure type Angular Blocky to Granular. Like stickiness, plasticity is directly
1230 related to the clay content (FAO, 2006). Horizons classified as “*Plastic OR*
1231 *Slightly plastic* AND Macropores size: *Very Fine (VF < 0.5 mm)*”, fit into the
1232
1233
1234
1235
1236
1237
1238
1239

1240
1241
1242 High B_d class, highlighting the link between high values of B_d and clay content
1243 (accuracy respectively of 100% and 66.7%).
1244
1245
1246
1247

- **Level 2: “Structure Type”: Prismatic → Level 3, “Void Abundance”
→ Level 4 ”Structure Grade” → Level 5: “Fissures”→ Level 6:
“Structure Size”**

1248
1249
1250
1251
1252
1253
1254 The “Prismatic” structure type is described by FAO, (2006) and by
1255 Schoeneberger et al. (2012) as having vertical elongated units with limited faces
1256 in the horizontal plane. Horizons having prismatic to angular blocky aggregates
1257 are classified by the model within the High B_d class (accuracy, 62.5%). The
1258 average depth ranges within 53-95 cm, classified across a number of soil types
1259 e.g. typical surface water gleys (Stagnosols reference soil group of the WRB),
1260 typical luvisols (Luvisols), typical brown podzolic (Podzols) and typical
1261 calcareous brown earths (Calcaric Cambisols). Different soil types are subjected
1262 to different mechanisms of soil particle aggregation which can exert a degree of
1263 compaction in a specific horizon, due to their intrinsic nature or to a
1264 combination of factors, such as: (i) clay concentrations in the impeded horizon,
1265 as for luvisols; (ii) translocation of Al and Fe in the spodic horizon, as for
1266 brown podzolic (Bronick and Lal, 2005; Collins, 2004), (iii) presence of
1267 carbonates, as for the calcareous brown earths (Boix-Fayos, et al., 2001) and
1268 (iv) presence of a poorly permeable horizon, as for the gleyic horizons in
1269 surface water gleys (Collins et al., 2004).
1270
1271
1272
1273
1274
1275
1276
1277
1278
1279
1280
1281
1282

1283 Furthermore, for the prismatic structure type, “**Voids abundance**” is selected as
1284 the main descriptor to split the data between High and Medium B_d for this
1285 structure type.
1286
1287
1288

1289 For the rules “Humose: *no*, AND Structure type: *Prismatic* AND Void
1290 abundance: *A, B, C*:

1291 (*A*) High (15-40%): the model returns 66.7% of correctly classified instances as
1292 belonging to the Medium B_d class,
1293
1294
1295
1296
1297
1298

1299
1300
1301
1302 (B) Very Low (<2%): the model classifies for the High B_d class with an
1303 accuracy of 75%.

1304
1305 (C) Medium (5-15%): the model classifies for Medium and High B_d with an
1306 accuracy of 83.3 and 89%, respectively.

1307
1308 The Low B_d category was not defined by the model for this structure type,
1309 indicating the prismatic arrangement as having overall higher B_d values. The
1310 abundance of voids is important, as the void size for this type of structure,
1311 poorer than the angular blocky structure type. Rules (A) and (B) associated
1312 higher void abundance with higher structure quality. On the other hand the rule
1313 (C), which took into account the medium void abundance category, requires
1314 further descriptors to categorise within the High and the Medium B_d classes,
1315 such as “**Structure grade**”, “**Fissures**” and “**Structure size**”.

1316
1317
1318
1319
1320 The presence of smaller sized prismatic aggregates (Structure size: *Fine 10-20*
1321 *mm*) directs the model to predict High B_d class with 100% correct instances. As
1322 found in the present study, the rapid wetting of dry soil which comes in contact
1323 with free water can cause micro-cracking. This increases ped friability, causing
1324 the production of smaller sized aggregates, which does not always result in
1325 lower values of B_d (Dexter, 2002).

1326
1327
1328
1329
1330
1331
1332
1333
1334
1335
1336
1337
1338
1339
1340
1341
1342
1343
1344
1345
1346
1347
1348
1349
1350
1351
1352
1353
1354
1355
1356
1357
Vertical fissures are also an important feature of this structure type. Although
hard clods are devoid of microstructure, fissures enable the percolation of the
surface water in the deeper layers (Russel et al., 1975). Such a drainage
advantage is not valid for the “Platy” structure type. In this case the model
returns two different outputs. Platy aggregates, probably formed by intensive
mechanical intervention, indicate compaction which affects water percolation,
resulting in high B_d values (accuracy, 66.7%). On the other hand, some platy
aggregates were attributed to the histic horizons (Of, Omf) which showed no
developed structure, associated with very low B_d (accuracy 75%).

1358
1359
1360
1361 • **Level 2: “Structure Type”: Massive**

1362 Structure types defined as “Massive” and “Single grain” were categorised by
1363 Schoeneberger et al. (2012) as structure less soils. Massive soil material
1364 normally has stronger consistence as the soil particles are arranged in a coherent
1365 mass and are very difficult to break (FAO, 2006). Horizons with “Massive”,
1366 “Massive to Angular blocky” and “Massive to Single Grain” structure types
1367 were classified by the model as belonging to the High B_d class with an accuracy
1368 of 77.8%, (n=63; very influential rule in the overall tree output), 83.4% and
1369 100%, respectively. Further analysis of the data showed that most of the
1370 horizons belonging to the rule: “Humose: *no*, AND Structure type: *Massive*”
1371 were described as having a hard or very hard consistence dry, fine or very fine
1372 macropores and very low void abundance. The decrease in soil macroporosity
1373 and the firm nature of the aggregates suggests a high level of compaction
1374 (Epron et al., 2016), resulting in high B_d values which ranged from 1.4 g cm⁻³ to
1375 1.9 g cm⁻³. In the case of the Massive to single grain structure type, “**Plasticity**”
1376 is a key attribute to assess the range of B_d (rule: “Humose: *no*, AND Structure
1377 type: *Massive to Single grain* AND Plasticity: *Non plastic*”).
1378
1379
1380
1381
1382
1383
1384
1385
1386
1387
1388
1389
1390
1391

1392 The arrangement of the aggregates which are weak and tend to disintegrate
1393 when sampling in the field, suggested the presence of sandy material held
1394 together in big, hard and massive aggregates. In some soils, sand grains have a
1395 film of orientated clay particles on the surface, not enough to be detected by
1396 feel, but that are able to strongly hold the sand particles packing them together
1397 in massive aggregates (Russel, 1975). Sandy soils are prone to compaction of
1398 surface layers, due to intensive agricultural operations (Ampoorter et al., 2007;
1399 Deconchat, 2001; Teepe et al., 2004).
1400

1401 Low B_d class was attributed by the model to the horizons responding to the rule
1402 “Humose: *no*, AND Structure type: *Single grain*”, which is a feature typical of
1403 sandy soils not subjected to compaction phenomena, thereby conserving a large
1404
1405
1406
1407
1408
1409
1410
1411
1412
1413
1414
1415
1416

1417
1418
1419 amount of wide pores (Ampoorter et al., 2007). The model correctly classified
1420 66.7% of the instances following this rule.
1421
1422
1423
1424

1425 **3.2 Model 2: Linear regression approach to predict a numerical estimate of** 1426 **B_d** 1427

1430 **3.2.1 Model and performance** 1431

1432 After several trials with different machine learning methods for numerical
1433 prediction, a linear regression model was selected based on better overall
1434 performance. This conclusion asserts that a strong linear relationship exists
1435 between the visual descriptors and B_d values. As a result, since the model
1436 produced by a linear regression algorithm is a linear equation, the predicted
1437 value of B_d can be easily computed in seconds without the need for time
1438 consuming and costly laboratory analyses.
1439
1440
1441
1442
1443
1444
1445
1446

1447 Model (2) considers only those descriptors that influence the final B_d value. For
1448 this quantitative estimation seven descriptors out of eleven were selected by the
1449 linear regression algorithm:
1450
1451
1452

- 1453 (i) Humose
 - 1454 (ii) Structure Grade
 - 1455 (iii) Structure Type
 - 1456 (iv) Structure Size
 - 1457 (v) Macropores
 - 1458 (vi) Void Size
 - 1459 (vii) Void Abundance
- 1460
1461
1462
1463
1464
1465
1466
1467
1468
1469
1470
1471
1472
1473
1474
1475

The linear equation produced by Model 2 to predict B_d is as follows:

$$\begin{aligned} B_d \text{ (g cm}^{-3}\text{)} = & \\ & 0.4575 * (\text{NO Humose: =true}) + \\ & -0.0517 * (\text{MODERATE Structure Grade=true}) + \\ & -0.2128 * (\text{GRANULAR Structure Type=true}) + \\ & 0.093 * (\text{MASSIVE Structure Type=true}) + \\ & -0.134 * (\text{SUBANGULAR BLOCKY Structure Type=true}) + \\ & -0.1501 * (\text{SUBANGULAR BLOCKY TO GRANULAR Structure Type=true}) + \\ & -0.1003 * (\text{ANGULAR BLOCKY TO GRANULAR Structure Type=true}) + \\ & -1.1619 * (\text{VERY COARSE > 10mm Structure Size=true}) + \\ & 0.1471 * (\text{VERY FINE < 0.5mm Macropores=true}) + \\ & -0.1791 * (\text{COARSE 5-20 mm Void Size=true}) + \\ & 0.0802 * (\text{VERY LOW Void Abundance=true}) + \\ & -0.0784 * (\text{HIGH Void Abundance=true}) + \\ & 0.8866 \end{aligned} \tag{Eq 10}$$

The equation produced follows a simple framework:

(i) All the descriptors associated with a *positive coefficient* caused a significant incremental increase in B_d . Basically, as the associated coefficients are positive, a soil classified having these descriptors ($V_i=1=true$, see description in paragraph 2.3.3), will result in an increased B_d final value.

The variables “*NOHumose=true*”, “*VERY FINE<0.5mm Macropores=true*”, “*VERY LOW Void Abundance=true*” and “*MASSIVE Structure Type=true*”, all cause an increase in B_d , with 0.4575; 0.1471; 0.0802; and 0.093 explanatory power, respectively.

1535
1536
1537
1538 In line with Model (1) results, the humification degree of OM has the greatest
1539 influence on B_d prediction. This characteristic, as well as readily defining B_d
1540 class, also informed small differences in soil B_d and generally indicated
1541 pedological features that were consistent with lower B_d values.
1542

1543
1544 Following the humic feature, macropores size was the second more
1545 discriminating feature, with the lower size able to distinguish a wide increment
1546 of prediction (multiplier of 0.1471). Furthermore, very low void abundance
1547 triggered the model as the fourth main attribute (multiplier of 0.0802). This was
1548 an expected result, as porosity was already investigated by the decision tree
1549 approach and was one of the most critical soil characteristics which took into
1550 account an evaluation of soil structure. In particular, size of pores was
1551 highlighted as a stronger predictor for an increase of B_d with respect to pore
1552 abundance. As seen from the decision tree output, the massive structure type has
1553 a role in increasing soil B_d . In general both models although operating at
1554 different scales produce the same descriptors for the prediction of B_d .
1555
1556
1557
1558
1559
1560
1561
1562
1563
1564
1565
1566

1567 (ii) All the descriptors associated with a *negative coefficient* have a role
1568 decreasing B_d . Basically, as the associated coefficients are negative, a soil
1569 classified as having these descriptors, resulted in a decreased B_d , and therefore
1570 have a better soil physical quality.
1571
1572
1573
1574
1575

1576 In Model (2), structure size appears to be a stronger descriptor which influences
1577 a decrease in B_d when evaluated as “*VERY COARSE > 10 mm Structure*
1578 *Size=true*” (multiplier of -1.1619). This was surprising considering that in
1579 Model (1) the size of aggregates was not particularly important (sixth level) in
1580 the tree hierarchy as a splitting attribute. This highlights that this feature is
1581 better at identifying small incremental reductions of B_d , but is less informative
1582 when splitting into wider B_d ranges.
1583
1584
1585
1586
1587
1588
1589
1590
1591
1592
1593

1594
1595
1596 However, in Model (2) Structure type still has to be considered one of the most
1597 informative variables, since it appears in four out of eight factors having a
1598 negative coefficient in the equation. In particular, looking at the equation, we
1599
1600
1601
1602 have:

- 1603 • “*GRANULAR Structure Type=true*” ,
- 1604 • “*SUBANGULAR BLOCKY TO GRANULAR Structure Type=true*” ,
- 1605 • “*SUBANGULAR BLOCKY Structure Type=true*” ,
- 1606 • “*ANGULAR BLOCKY TO GRANULAR Structure Type=true*” ,
- 1607
- 1608
- 1609

1610 as coefficients -0.2128; -0.1501; -0.134; -0.1003, respectively.

1611
1612 Granular structure type is responsible of a higher decrease of B_d , confirming
1613 what was found for Model (1), indicating good soil structure.

1614
1615
1616
1617
1618 The model showed sufficient sensitivity allowing the identification of
1619 differences related to soil structure type. This is despite the relatively crude
1620 measurement of soil structure at field level in tandem with other attributes. In
1621 particular while the soil structure quality, associated with a change of structure
1622 type, gradually decreases, with diminishing negative effect on B_d , indicated by
1623 the coefficients for individual structure types. Hence, corresponding to their
1624 respective coefficients, a granular structure type will have a higher negative
1625 increment, resulting in a reduction of the B_d final value, while an angular blocky
1626 to granular structure type will have a lower negative reduction in the final
1627 predicted value, resulting in a higher B_d final value.

1628
1629
1630
1631
1632
1633
1634
1635
1636
1637
1638 Structure size, Void size, Void abundance and Structure grade were, in order of
1639 importance, the next most informative features for the linear regression model.

1640
1641
1642 If both the features relating to porosity appear in the Model (1) at a high level in
1643 the tree hierarchy (level 3), for this model only void size with the variable
1644 “*COARSE 5-20 mm Void Size=true*” appears to have higher negative impact,
1645 with a relatively high coefficient of -0.1791, while void abundance (*HIGH Void*
1646
1647
1648
1649
1650
1651
1652

1653
1654
1655
1656 *Abundance=true*) resulted in having less negative impact on the definition of a
1657 final B_d value, being associated with a smaller coefficient, -0.0784. Probably, as
1658 per the decision tree model, the shape of aggregates is again a critical point
1659 which drives the selection of the second decisive node into pore abundance or
1660 size, depending on the original structure type.
1661
1662
1663
1664
1665
1666

1667 **3.2.2 Overall model evaluation**

1668
1669 The overall correlation coefficient on training set for the linear regression model
1670 is 0.71 with Root Mean Squared Error (RMSE): 0.25 and Mean Absolute Error
1671 (MAE): 0.20; (Table 4). After a 10-fold cross validation the correlation
1672 coefficient slightly dropped, to 0.65, with similar error ranges (RMSE: 0.27 and
1673 MAE: 0.21); (Table 4). The errors reported for this model may be considered
1674 quite high in relation to a standard lab-based B_d measure. However, it is
1675 important to highlight that the model has been fed using only soil visual
1676 parameters. Considering the nature of these data inputs and the influence that
1677 different operators can have during the classification phase, this range of error is
1678 low.
1679
1680
1681
1682
1683
1684
1685
1686

1687 **Figure 4-2** shows the prediction performances of Model (2). The distribution of
1688 predicted values results more coherent with the real values for a middle range of
1689 B_d values. In particular we identified a range that goes between 0.8 to 1.6 g cm⁻³,
1690 **which falls within the typical range of B_d found in Irish grassland soils**, where
1691 the model returns B_d values close to real values. In these cases the model is
1692 more robust, predicting a numerical estimate with a quite low standard error.
1693 Furthermore, neither overestimation nor underestimation prevails for a middle
1694 range of B_d .
1695
1696
1697
1698
1699
1700

1701 The model shows the higher errors for the extreme B_d classes, namely (i) very
1702 low B_d , that we identified as values lower than 0.8 g cm⁻³, or (ii) very high B_d
1703 values, identified as values higher than 1.6 g cm⁻³. The algorithm appears to a
1704 have higher prediction power on medium B_d values, **which fall within the**
1705
1706
1707
1708
1709
1710
1711

1712
1713
1714
1715 ~~typical range of B_d found in Irish grassland soils, and hence, also~~ which also
1716 receive higher representation in our dataset. In general, machine learning
1717 algorithms are improved where greater input data is provided. Therefore, in our
1718 case, the algorithm is inherently biased towards the correct prediction of
1719 medium ranges.
1720
1721
1722
1723

1724 1725 **3.3 Models choice considerations**

1726
1727 We have chosen to use decision trees and linear regression because these simple
1728 types of models allow users to identify the B_d class (for decision trees), and the
1729 B_d value (for linear regression) without the need to rely on additional software.
1730
1731 Furthermore, besides the predictive ability, decision trees also provide
1732 descriptive power, in that they make explicit the relationships among different
1733 characteristics of the soils and allow the user to have greater insight to these
1734 relationships. Other algorithms that were considered, i.e., support vector
1735 machines and multi-layer perceptron, although leading to similar performance,
1736 do not allow this type of insight. A full comparison between different
1737 algorithms, from the performance point of view, can be conducted in future.
1738 While the quality of the interrogated database was good, we believe that further
1739 improvement of model performance can be achieved by increasing the extent of
1740 the sample dataset, especially for horizons with low and high B_d values, which
1741 are less represented in our data. Finally, the utility of these models to assess
1742 critical thresholds for compaction should be evaluated for descriptive soil
1743 datasets where attributes such as “Compact degree” (FAO, 2006) are included.
1744
1745
1746
1747
1748
1749
1750
1751
1752
1753
1754
1755
1756
1757

1758 1759 **4. Conclusion**

1760
1761 A decision tree and linear equation model were developed to predict soil bulk
1762 density on the basis of visual descriptors. The visual soil descriptors identified,
1763 as being more informative by both models, are associated with specific soil
1764 properties. This allows the user to rank to these properties in terms of their
1765
1766
1767
1768
1769
1770

1771
1772
1773
1774
1775
1776
1777
1778
1779
1780
1781
1782
1783
1784
1785
1786
1787
1788
1789
1790
1791
1792
1793
1794
1795
1796
1797
1798
1799
1800
1801
1802
1803
1804
1805
1806
1807
1808
1809
1810
1811
1812
1813
1814
1815
1816
1817
1818
1819
1820
1821
1822
1823
1824
1825
1826
1827
1828
1829

impact on soil structural quality. For both models the most relevant properties that affect B_d appears to be soil humic characteristics, followed by soil porosity and pedogenic formation.

Overall, the decision tree model shows an accuracy of about 60%, while the linear equation model had a correlation coefficient of about 0.65 with respect to the measured B_d values. The two models are parsimonious and can be used by soil surveyors and analysts who need to have a quick and approximate *in-situ* estimate of the structural quality for various soil functional applications. Furthermore they have an enormous potential to retrofit B_d data (i.e. gap fill) to existing data sets where laboratory data are missing. Future work is required to refine these models for use on soils with very low and very high B_d classes which fall outside those typically found in Ireland. Finally, our goal is to encode the decision tree and the linear equation into a mobile application, in order to enable multiple user types to perform B_d prediction more quickly, on site, and in a user friendly manner.

Acknowledgements

The authors thank Irene Marongiu for her help with the physical and chemical soil analyses. SQUARE project has received funding from the Irish Department of Agriculture (DAFM) Research Stimulus Fund (RSF). Task 3 output.

References

- Alvarez, S.A., 2002. An exact analytical relation among recall, precision, and classification accuracy in information retrieval. Tech. Rep. BCCS-02-01, Computer Science Department, Boston College.
- Ampoorter, E., Goris, R., Cornelis, W. M., Verheyen, K., 2007. Impact of mechanized logging on compaction status of sandy forest soils. *Forest Ecol. Manag.* 241, 162–174.

- 1830
1831
1832
1833 Armino, R.A., Wendroth, O. 2016. Physical soil structure evaluation based on
1834 hydraulic energy functions. *Soil Sci. Am. J.* 80, 1167–1180.
1835
1836 Attou, F., Bruand, A., Bissonnais, Y. L., 1998. Effect of clay content and silt-
1837 clay fabric on stability of artificial aggregates. *Eur. J. Soil Sci.* 49, 569–577.
1838
1839 Ball, B. C., Munkholm, L. J., 2015. *Visual Soil Evaluation: Realizing Potential*
1840 *Crop Production with Minimum Environmental Impact.* CAB International.
1841 London.
1842
1843
1844 Batey, T., 2000. Soil profile description and evaluation. In: Smith, K., Mullins,
1845 C. (Eds.), *Soil and environmental analysis, physical methods*, 2nd edition.
1846 Marcel Dekker, New York. pp. 595–628
1847
1848
1849 Bhargava, N., Sharma, G., Bhargava, R., Mathuria, M., 2013. Decision tree
1850 analysis on j48 algorithm for data mining. *Proceedings of International*
1851 *Journal of Advanced Research in Computer Science and Software*
1852 *Engineering.* 3, 1114–1119.
1853
1854
1855 Boix-Fayos, C., Calvo-Cases, A., Imeson, A.C., 2001. Influence of soil
1856 properties on the aggregation of some Mediterranean soils and the use of
1857 aggregate size and stability as land degradation indicators. *Catena* 44, 47–67.
1858
1859
1860 Bronick, C. J., Lal, R. 2005. Soil structure and management: a review.
1861 *Geoderma.* 124, 3–22.
1862
1863
1864 Caravaca, F., Hernandez, T., Garcia, C., Roldan, A., 2002. Improvement of
1865 rhizosphere aggregate stability of afforested semiarid plant species subjected
1866 to mycorrhizal inoculation and compost addition. *Geoderma.* 108, 133–144.
1867
1868
1869 Collins, J. F., Larney, F. J., Morgan, M. A., 2004. Climate and soil
1870 management, in: Keane, T., Collins, J. F. (Eds.), *Climate, Weather and Irish*
1871 *Agriculture. Working group on Applied Agricultural Meteorology*
1872 *(AGMET), Dublin,* pp. 119–160.
1873
1874
1875 Creamer, R., Simo, I., Reidy, Carvalho, J., Fealy, R., Hallett, S., Jones, R.,
1876 Holden, A., Holden, N., Hannam, J., Massey, P., Mayr, T., McDonald, E.,
1877 O'Rourke, S., Sills, P., Truckell, I., Zawadzka, J., Schulte, R., 2014. *Irish*
1878 *Soil Information System. (2007-S-CD-1-S1) EPA STRIVE Programme*
1879 *2007–2013, Synthesis Report.*
1880
1881
1882
1883
1884
1885
1886
1887
1888

- 1889
1890
1891
1892 Dam, R.F., Mehdi, B.B., Burgess, M.S.E., Madramootoo, C.A., Mehuys, G.R.,
1893 Callum, I.R., 2005. Soil bulk density and crop yield under eleven
1894 consecutive years of corn with different tillage and residue practices in a
1895 sandy loam soil in central Canada. *Soil Till. Res.* 84, 41–53.
1896
1897
1898 Deconchat, M., 2001. Effets des techniques d'exploitation forestie`res sur
1899 l'e'tatde surface du sol. *Ann. For. Sci.* 58, 653–661.
1900
1901 Dexter, A. R., 1988. Advances in characterization of soil structure, *Soil Till.*
1902 *Res.* 11, 199–238.
1903
1904 Dexter, A. R., 2002. Soil structure: the key to soil function, in: Pagliai, M.,
1905 Jones, R., (Eds.), *Sustainable land Management – Environmental Protection,*
1906 *a soil Physical Approach. Advances in Geocology 35,* Clearance Center,
1907 Inc., Reiskirchen, pp. 57–69.
1908
1909
1910 Ellert, B. H., Bettany, J. R., 1995. Calculation of organic matter and nutrient
1911 stored in soils under constrain management regimes. *Can. J. Soil Sci.* 75,
1912 529–538.
1913
1914
1915 Emmet-Booth, J. P., Forristal, P. D., Fenton, O., Ball, B. C., Holden, N. M.,
1916 2016. A review of visual soil evaluation techniques for soil structure. *Soil*
1917 *Use Manage.* 32, 623–634.
1918
1919
1920 Epron, D., Plain, C., Ndiaye, F. K., Bonnaud, P., Pasquier, C., Ranger, J., 2016.
1921 Effects of compaction by heavy machine traffic on soil fluxes of methane
1922 and carbon dioxide in a temperate broadleaved forest. *Forest Ecol. Manag.*
1923 382, 1–9.
1924
1925
1926
1927
1928
1929
1930
1931
1932
1933
1934
1935
1936
1937
1938
1939
1940
1941
1942
1943
1944
1945
1946
1947

- 1948
1949
1950
1951 Geissen, V., Kampichler, C., López-de Llergo-Juárez, J. J., Galindo-Acántara,
1952 A., 2007. Superficial and subterranean soil erosion in Tabasco, tropical
1953 Mexico: development of a decision tree modeling approach. *Geoderma*. 139,
1954 277–287.
1955
1956
1957 Håkansson, I., Lipiec, J., 2000. A review of the usefulness of relative bulk
1958 density values in studies of soil structure and compaction. *Soil Till. Res.* 53,
1959 71–85.
1960
1961
1962 Haynes, R.J., Naidu, R., 1998. Influence of lime, fertilizer and manure
1963 applications on soil organic matter content and soil physical conditions: a
1964 review. *Nutr. Cycl. Agroecosyst.* 51, 123–137.
1965
1966
1967 Henderson, B. L., Bui, E. N., Moran, C. J., Simon, D. A. P., 2005. Australia-
1968 wide predictions of soil properties using decision trees. *Geoderma*. 124, 383–
1969 398.
1970
1971
1972 Holden, N., Brereton, A.J., 2004. Definition of agroclimatic regions in Ireland
1973 using hydro-thermal and crop yield data. *Agr. Forest Meteorol.* 122, 175–
1974 191.
1975
1976
1977 IUSS Working Group WRB, 2006. World Reference Base for Soil Resources –
1978 a framework for international classification, correlation and communication.
1979 World Soil Resources Reports 103. FAO, Rome.
1980
1981
1982 Jin, R., Li, X., Che, T., 2009. A decision tree algorithm for surface soil
1983 freeze/thaw classification over China using SSM/I brightness temperature.
1984 *Remote Sens. Environ.* 113, 2651–2660.
1985
1986
1987 Karlen, D.L., 2004. Soil quality as an indicator of sustainable tillage practices.
1988 *Soil Till. Res.* 78, 129–130.
1989
1990
1991 Kaur, R., Sanjeev, K., Gurung, H., 2002. Apedo-transfer function (PTF) for
1992 estimating soil bulk density from basic soil data and its comparison with
1993 existing PTFs. *Aust. J. Soil Res.* 40, 847–857.
1994
1995
1996 Kay, B.D., 1998. Soil structure and organic carbon: a review. In: Lal, R.,
1997 Kimble, J.M., Follett, R.F., Stewart, B.A. (Eds.), *Soil Processes and the*
1998 *Carbon Cycle*. CRC Press, Boca Raton, pp. 169-197.
1999
2000
2001 Kay, B.D., Hajabbasi, M.A., Ying, J., Tollenaar, M., 2006. Optimum versus
2002 non-limiting water contents for root growth, biomass accumulation, gas
2003
2004
2005
2006

- 2007
2008
2009
2010
2011
2012
2013
2014
2015
2016
2017
2018
2019
2020
2021
2022
2023
2024
2025
2026
2027
2028
2029
2030
2031
2032
2033
2034
2035
2036
2037
2038
2039
2040
2041
2042
2043
2044
2045
2046
2047
2048
2049
2050
2051
2052
2053
2054
2055
2056
2057
2058
2059
2060
2061
2062
2063
2064
2065
- exchange and the rate of development of maize (*Zea mays* L.). *Soil Till. Res.* 88, 42–54.
- Lee, K. E., Foster, R. C., 1991. Soil fauna and soil structure. *Aust. J. Soil Res.* 29, 745–775.
- Leonavičiutė, N., 2000. Predicting soil bulk and particle densities by pedotransfer functions from existing soil data in Lithuania, *Geografijos metraštis*. 33, 317–330.
- Logsdon, S.D., Karlen, D.L., 2004. Bulk density as a soil quality indicator during conversion to no-tillage. *Soil Till. Res.* 78, 143–149.
- Moncada, M.P., Ball, B.C., Gabriels, D., Lobo, D. and Cornelis, W.M., 2015. Evaluation of soil physical quality index S for some tropical and temperate medium-textured soils. *Soil Sci. Soc. America J.* 79, 9–19
- Mueller, L., Kay, B. D., Deen, B., Hu, C., Zhang, Y., Wolff, M., Eulenstein, F., Schindler, U., 2009. Visual assessment of soil structure: Part II. Implications of tillage, rotation and traffic on sites in Canada, China and Germany. *Soil Till. Res.* 103, 188–196.
- Pachepsky, Y. A., Rawls, W. J., 2003. Soil structure and pedotransfer functions. *Eur. J. Soil Sci.* 54, 443–452.
- Pagliai, M., Vignozzi, N., 2002. The soil pore system as an indicator of soil quality, in: Pagliai, M., Jones, R., (Eds.), *Sustainable land Management – Environmental Protection, a soil Physical Approach*. *Advances in Geocology* 35, Clearance Center, Inc., Reiskirchen, pp. 71–82.
- Quinlan, J. R., 1993. *C4.5: Programs for Machine Learning*. Morgan Kaufmann Publishers.
- Reidy, B., Simo, I., Sills, P., Creamer, R. E., 2016. Pedotransfer functions for Irish soils-estimation of bulk density (ρ_b) per horizon type. *Soil*. 2, 25–39.
- Russell, E. W., 1975. *Soil Conditions and Plant Growth* 10th edition. Ed. Longman, London.
- Saffih-Hdadi, K., Défossez, P., Richard, G., Cui, Y. J., Tang, A. M., Chaplain, V., 2009. A method for predicting soil susceptibility to the compaction of

2066
2067
2068 surface layers as a function of water content and bulk density, *Soil Till. Res.*
2069 105, 96–103.
2070
2071

2072 Schoeneberger, P.J., D.A. Wysocki, E.C. Benham, and Soil Survey Staff. 2012.
2073 Field book for describing and sampling soils, Version 3.0. Natural Resources
2074 Conservation Service, National Soil Survey Center, Lincoln, NE.
2075
2076

2077 Schulten, H.R., Leinweber, P., 2000. New insights into organic– mineral
2078 particles: composition, properties and models of molecular structure. *Biol.*
2079 *Fertil. Soils.* 30, 399– 432.
2080
2081

2082 Shipitalo, M. J., Le Bayon, R. C., 2004. 10 Quantifying the Effects of
2083 Earthworms on Soil Aggregation and Porosity, in: Edwards, C.A. (Eds.)
2084 Earthworm ecology 2nd edition, Boca Raton, pp 183–199.
2085
2086

2087 Soil Survey Division Staff, 1993. Soil Survey Manual. Agricultural Handbook
2088 N 18. USDA Natural Resources Conservation Service, Washington D.C.
2089
2090

2091 Stevenson, F.J. 1994. Humus chemistry. genesis, composition, reactions. 2nd
2092 edition. Wiley Interscience, New York.
2093
2094

2095 Teepe, R., Brumme, R., Beese, F., Ludig, B., 2004. Nitrous oxide emission and
2096 methane consumption following compaction of forest soils. *Soil Sci. Soc.*
2097 *Am. J.* 68, 605–611.
2098
2099

2100 Templ, M., Kowarik, A., & Filzmoser, P., 2011. Iterative stepwise regression
2101 imputation using standard and robust methods. *Comput. Stat. Data An.* 55,
2102 2793–2806.
2103
2104

2105 Xue, D., De Baets, B., Van Cleemput, O., Hennessy, C., Berglund, M., Boeckx,
2106 P., 2013. Classification of nitrate polluting activities through clustering of
2107 isotope mixing model outputs. *J. Environ. Qual.* 42, 1486–1497.
2108
2109

2110 Xue, D., Pang, F., Meng, F., Wang, Z., Wu, W., 2015. Decision-tree-model
2111 identification of nitrate pollution activities in groundwater: A combination of
2112 a dual isotope approach and chemical ions. *J. Contam. Hydrol.* 180, 25–33.
2113
2114
2115
2116
2117
2118
2119
2120
2121
2122
2123
2124

Table 1. Selection of soil structure field descriptors described by FAO, Guidelines for Soil Description, 2006.

Descriptor	Title	Description
1	Humose	This is an estimation of the degree of humification of the organic material. Surveyor must provide a positive or affirmative answer to being humose (this descriptor was recorded as a presence/absence in the database).
2	Soil Consistency	The strength with which soil materials are held together. It provides a means of describing the degree of cohesion and adhesion between the soil particles as related to the resistance of the soil to deform or rupture. It includes soil properties such as friability, plasticity, stickiness and resistance to compression. It changes with soil moisture and is highly related to the percentage of clay and OM in the soil.
3	Stickiness	It is the capacity of the soil to adhere to an object. It is evaluated pressing a small amount of wet soil between thumb and forefinger to see if it will stick to fingers.
4	Plasticity	The ability of soil material to retain a shape after pressure deformation. It is evaluated by rolling a small amount of wet soil between the hand palms until it forms a long, round strip like a wire about 3 mm thick.
Soil structure* is described as the combination of (5, 6, 7)		
5	Structure Grade	It describes the level of development of soil structure. It is expressed as the differential between cohesion within aggregates and adhesion between aggregates. It is evaluated in relation to the arrangement of the aggregates and to the strength necessary to break them.
6	Structure Type	It describes the form or shape of individual aggregates and is directly correlated with the pedogenic formation.
7	Structure Size	It describes the average size of individual aggregates. Different classes may be recognized in relation to the type of soil structure from which they come.
Voids** is described as the combination of (8, 9)		
8	Voids Abundance	An indication of the total volume of voids measured by area and was recorded as the percentage of the surface occupied by pores.
9	Voids Size	The diameter of voids and was recorded in mm.
10	Fissures size	The diameter of fissures and was recorded in mm.
11	Macropores size	The diameter of macropores, which are described as bigger void, mostly determined by plant roots, and by zoological exploration. Macropores were recorded in mm.
*Soil Structure: It refers to the spatial disposition of aggregates which are the result of the aggregation of single particles such as sand, silt and clay. Size, shape and arrangement of these solids and voids, determining the porosity and the capacity to retain fluids and inorganic and organic substances can occur in different patterns, resulting in different soil structures (Bronick et Lal, 2005).** Voids: Include all the pore space present in the soil. It is closely related to the porosity and is a good indicator of soil compactness. It is evaluated as presence/absence data. Voids were described in terms of size and abundance.		

Table 2. Decision tree model (Model 1); performances. RMSE: Root Mean Squared Error; MAE: Mean Absolute Error

	Performance with cross validation				Performance on training set			
	N. of instances	Accuracy	RMSE	MAE	N. of instances	Accuracy	RMSE	MAE
Correctly Classified Instances	283	60.08 %	0.44	0.32	335	71.12%	0.37	0.27
Incorrectly Classified Instances	188	39.91 %			136	28.87 %		
	N. of instances	Precision	Recall	F-measure	N. of instances	Precision	Recall	F-measure
Low B_d class	137	0.70	0.54	0.60	137	0.75	0.65	0.69
Medium B_d class	178	0.53	0.63	0.58	178	0.64	0.73	0.68
High B_d class	156	0.62	0.62	0.62	156	0.76	0.74	0.75
Weighted Average		0.61	0.60	0.60		0.72	0.71	0.71

Table 3. Decision tree model (Model 1); confusion matrix.

Classes classified by decision tree model (N. of instances=471)			
	a	b	c
Low B_d class (a)	74	46	17
Medium B_d class (b)	25	112	41
High B_d class (c)	7	52	97

Table 4. Linear regression model (Model 2); performances. RMSE: Root Mean Squared Error; MAE: Mean Absolute Error

	Performance with cross validation				Performance on training set			
	N. of instances	Correlation coefficient	RMSE	MAE	N. of instances	Correlation coefficient	RMSE	MAE
Instances	471	0.65	0.27	0.21	471	0.71	0.25	0.20

1
2
3
4 **Highlights:**
5

- 6 • **Two models to estimate B_d values based on soil visual descriptors, are**
7 **proposed.**
8
- 9 • **Machine learning techniques were used to build the models.**
10
- 11 • **Estimation of B_d by these models can replace complex laboratory**
12 **analysis.**
13
- 14 • **Relevant properties affecting soil B_d are humic feature, porosity and**
15 **pedogenesis.**
16
17
18
19
20
21
22
23
24
25
26
27
28
29
30
31
32
33
34
35
36
37
38
39
40
41
42
43
44
45
46
47
48
49
50
51
52
53
54
55
56
57
58
59

1
2
3
4 **Using machine learning to predict soil bulk density on the basis of visual**
5 **parameters: tools for in-field and post-field evaluation**
6
7

8 **Giulia Bondi^{a*}, Rachel Creamer^b, Alessio Ferrari^c, Owen Fenton^a, David**
9 **Wall^a**
10

11
12 *^aTeagasc Crops, Environment and Land-Use Research Centre, Wexford, Ireland;*

13
14 *^bSoil Biology and Biological Soil Quality, Wageningen University, Wageningen, The*
15 *Netherlands;*

16
17 *^cConsiglio Nazionale delle Ricerche, Istituto di Scienza e Tecnologie dell'Informazione "A.*
18 *Faedo" (CNR-ISTI), Pisa, Italy.*

19
20
21
22
23 ***Corresponding author:** G. Bondi (Email: Giulia.Bondi@teagasc.ie)

24
25 R. Creamer (Email: rachel.creamer@wur.nl); A. Ferrari (Email: alessio.ferrari@isti.cnr.it);

26
27 O. Fenton (Email: Owen.Fenton@teagasc.ie); D. Wall (Email: David.Wall@teagasc.ie).
28
29
30
31

32 **Abstract**
33

34 Soil structure is a key factor that supports all soil functions. Extracting intact
35 soil cores and horizon specific samples for determination of soil physical
36 parameters (e.g. bulk density (B_d) or particle size distribution) is a common
37 practice for assessing indicators of soil structure. However, these are often
38 difficult to measure, since they require expensive and time consuming
39 laboratory analyses. Our aim was to provide tools, through the use of machine
40 learning techniques, to estimate the value of B_d based solely on soil visual
41 assessment, observed by operators directly in the field. The first tool was a
42 decision tree model, derived through a decision tree learning algorithm, which
43 allows discrimination amongst three B_d ranges. The second tool was a linear
44 equation model, derived through a linear regression algorithm, which predicts
45 the numerical value of soil B_d . These tools were validated on a dataset of 471
46
47
48
49
50
51
52
53
54
55
56
57
58
59

60
61
62 soil horizons, belonging to 201 soil profile pits surveyed in Ireland. Overall, the
63 decision tree model showed an accuracy of ~60%, while the linear equation
64 model has a correlation coefficient of about 0.65 compared to the measured B_d
65 values. For both models, the most relevant property affecting soil structural
66 quality appears to be the humic characteristics of the soil, followed by soil
67 porosity and pedogenic formation. The two tools are parsimonious and can be
68 used by soil surveyors and analysts who need to have an approximate in-situ
69 estimate of the structural quality for various soil functional applications.
70
71
72
73
74
75
76
77
78
79
80

81 **Keywords:** soil bulk density, soil structure, soil quality, machine learning
82
83
84
85

86 **1. Introduction**

87

88 The importance of soil structure in relation to soil quality is well known
89 (Mueller et al., 2009; Karlen, 2004; Kay et al., 2006). A commonly used soil
90 physical measurement to characterize soil structural quality is soil bulk density
91 (B_d) (Armino and Wendroth, 2016; Dam et al., 2005; Håkansson and Lipiec,
92 2000; Logsdon and Karlen, 2004; Moncada et al., 2015), which is defined as the
93 oven-dry mass per unit volume of soil (IUSS Working Group, 2006; Mueller et
94 al., 2009). Measurement of soil B_d is useful as it describes both the packing
95 structure of the soil and its permeability (Dexter, 1988), whereby drainage
96 characteristics can be inferred (Reidy et al., 2016). B_d measurement is often
97 used in agronomic studies as it indicates the presence of compacted layers
98 resulting from machinery or animal traffic (Reidy et al., 2016; Saffih-Hdadi,
99 2009), which may affect crop production. It is commonly considered an
100 efficient measurement of soil carbon and nutrient stocks (Ellert and Bettany,
101 1995; Reidy et al., 2016).
102
103
104
105
106
107
108
109
110
111
112
113
114
115
116
117
118

119
120
121
122 However, the process of measuring B_d is often time consuming and open to
123 human bias in the field and requires accurate laboratory analyses using trained
124 personnel. Furthermore, soil texture has an important influence on the
125 assessment of B_d e.g. in soils with high clay or sand content, or very humic
126 soils, it may be difficult to obtain a representative sample and large variability
127 between replicate samples can represent a problem. Also, in some soils the
128 presence of stones can make sampling almost unmanageable. For such reasons,
129 or constraints of budget or laboratory facilities, B_d measurements are commonly
130 missing from soil databases (Reidy et al., 2016).
131
132
133
134
135
136
137
138

139 The main methods employed for the prediction of B_d are pedotransfer functions
140 (PTF) methods, based on measurable soil attributes, such as organic carbon
141 (OC) and clay content (Kaur et al., 2002; Leonavičiūtė, 2000; Reidy et al.,
142 2016). However, many of these methods ignore horizonation and depth
143 variances for soil B_d prediction (Reidy et al., 2016). Furthermore, the nature of
144 these methods, based on chemical/physical or landscape parameters, do not
145 capture the intrinsic nature of the soil structural properties.
146
147
148
149
150
151
152

153 Our experience with respect to soil descriptions and classification has shown
154 that the visual observations collected in the field at horizon level are often very
155 important for the evaluation of soil quality (Fenton et al., 2017; 2015) and they
156 become essential during the interpretation of the trend of some analytical
157 parameters used as indicators of soil structure status e.g. B_d .
158
159
160
161

162 Soil structural quality has been assessed visually for millennia (Batey, 2000)
163 e.g. soil survey manuals used in the field such as the Soils Survey Division Staff
164 Manual (1993) or the WRB for soil resources (FAO, ISRIC and ISSS, 1998)
165 include soil structure visual observations. However, soil scientists, for a long
166 time, have presented repeatable procedures for the examination of soil structural
167
168
169
170
171
172
173
174
175
176
177

178
179
180 form, stability and resilience (see latest review by Emmet-Booth et al., 2016
181 with examples from 1940's to present; Ball and Munkholm, 2015).
182
183
184

185 Taking this into account, in the present work we investigated whether, and to
186 what extent those visual observations, called descriptors, can be used to predict
187 soil B_d , which is considered one of the most efficient indicators in the
188 assessment of soil structure quality (Moncada et al., 2015).
189
190
191

192
193 In order to achieve this objective, machine learning techniques were used. The
194 potential of machine learning techniques have been rediscovered in the last few
195 years through various applications in environmental sciences.
196
197
198

199 Worldwide, decision tree approaches have been used for different purposes:
200 identifying sources of soil pollution (Xue et al., 2015); describing the extension
201 of different forms of soil erosion in Mexico (Geissen et al., 2007); predicting
202 chemical soil properties at national level in Australia (Henderson et al., 2005);
203 classifying the surface soil freeze/thaw status in China (Jin et al., 2009) and
204 even studying of soil structure through the prediction of soil hydraulic
205 properties (Pachepsky and Rawls, 2003). However, limited literature has been
206 found on the use of these powerful tools for environmental science in Europe.
207
208
209
210
211
212
213
214

215 The decision tree model output applied in this paper is based on a series of rules
216 generated by the software, which can be visualised as paths starting from the
217 root of the decision tree and ending at one of the leaves (Bhargava et al., 2013;
218 Xue et al., 2013; Xue et al., 2015). Each of those paths corresponds to one or
219 more soil *descriptors*, which are related to an internal *node* (Henderson et al.,
220 2005). The model is able to examine all possible descriptors and then to select
221 the most decisive *splitting attribute* (Xue et al., 2013). This operation occurs
222 several times until all the instances are correctly classified in a set of *rules*. Each
223 descriptor included in the model corresponds to a more defined *level* of
224 classification.
225
226
227
228
229
230
231
232
233
234
235
236

237
238
239 The linear regression model applied in this paper is a classical statistical
240 technique used to predict numerical data. It is based on the modelling of the
241 relationship between a scalar dependent variable and one or more explanatory
242 variables.
243
244
245
246
247

248
249 With our work we want to:

250
251 (i) Provide an operational strategy to estimate a range of B_d values, based on the
252 visual soil parameters by means of a decision tree approach. This model can be
253 used as a field tool to predict a general class of B_d (Low, Medium and High). It
254 is an instrument able to discriminate between macro classes and has to be
255 considered as a descriptive tool for *qualitative* estimation.
256
257
258
259

260
261 (ii) Propose an algorithm that can predict a numerical estimate of B_d . This
262 second model should discriminate better between smaller increments. This
263 instrument has to be considered as a more refined tool for *quantitative*
264 estimation.
265
266
267
268
269

270 **2. Methods**

271 **2.1 Primary data source and descriptors**

272
273 Two pedological surveys, where full soil profile descriptions and supporting
274 laboratory analyses, were carried out in Ireland with the aim of defining a
275 coherent and homogeneous way to study soil formation, functions and quality:
276
277
278

- 279
280 1. The Irish Soil Information System (Irish SIS) project was established in
281 2008. It aimed to conduct a programme of structured research into the
282 national distribution of soil types and construct a soil map, at 1:250,000
283 scale, able to identify and describe the soils according to a harmonised
284 national legend. Irish SIS included more than 225 sites distributed around
285 Ireland (Creamer et al., 2014).
286
287
288
289
290
291
292
293
294
295

- 296
297
298
299
300
301
302
303
304
305
306
307
308
309
2. The Soil Quality and Research project (SQUARE) started in 2013. The aim was to establish a baseline of soil quality in Ireland. The SQUARE soil survey included 38 grassland sites distributed within the five major agro climatic regions of Ireland defined by Holden and Bereton (2004) and classified into two drainage classes on the basis of the Irish Soil classification System.

310
311
312
313
314
315
316
317
318
319

During both (1) and (2) profile pits approximately 1 m deep, were observed and described by different operators. For the present study data from 201 profiles (168 Irish SIS, 33 SQUARE) was extracted from the larger database to cover a wide variety of Irish soil types with a specific focus on mineral soils. This data represents 471 horizons (<http://gis.teagasc.ie/soils/map.php>).

320
321
322
323
324
325
326
327
328
329
330
331
332
333
334
335
336
337
338
339
340
341
342
343

Although different surveyors worked across the projects mentioned, a systematic procedure was applied to describe the nature of the soil profiles, which included each of the soil horizons. Training was given to field operators. Using knowledge of soil structure and quality, the operators followed a widely understood schema of observation (developed by FAO through the Guidelines for Soil Description in 2006) which was able to investigate and finally characterize soil structure through visual parameters (FAO, 2006; FAO, ISRIC and ISS, 1998). Herein we have selected eleven descriptors presented in Table 1 (justifications are provided in Table 1), which may be considered the most important for the qualitative judgment of soil structure. Each descriptor was described and recorded on the basis of a set of pre-defined categories, reported in Table 1 in the Supplementary Material.

344 345 346

2.2 Soil analysis

347
348
349
350
351
352
353
354

The procedure to determine B_d of intact cores is a version of the ISO 11272:1998 – Soil Quality Part 5: Physical methods Sect. 5.6 – Determination of dry bulk density. The primary difference between the ISO and the applied

355
356
357 methodology is that the ISO does not account for stone mass and volume in its
358 core method, whereas the methodology applied in this study includes the
359 following equation to calculate B_d (stone free):
360
361
362
363

$$364 \quad B_d \text{ (g cm}^{-3}\text{)} = (Md - Ms)/(V - Vs) \quad \text{Eq 1}$$

365
366
367 where; Md: oven dry soil material weight (g), Ms: oven dry stone weight (g), V:
368 volume of soil core (cm^{-3}), Vs: volume of stones (mL). Soil B_d values reported
369 in this paper correspond to the mean of the three values obtained for each
370 horizon sampled.
371
372
373
374
375
376
377

378 **2.3 Model frameworks**

379 Two models were built by means of the modelling tool WEKA (Waikato
380 Environment for Knowledge Analysis). WEKA 3.8 is open source software for
381 machine learning and data mining under the General public license developed at
382 the University of Waikato in New Zealand
383 (<http://www.cs.waikato.ac.nz/ml/weka>, Bhargava et al., 2013). This software
384 includes different implementations of several machine learning algorithms. In
385 our context, we used two specific algorithms that are made available by the tool,
386 namely:
387
388
389
390
391
392
393

- 394 • the j48 algorithm, which corresponds to the WEKA's implementation of the
395 C4.5 decision tree learner (Quinlan, 1993; Xue et al., 2015) which was used
396 to build Model (1);
397
398
- 399 • a linear regression algorithm, used to build the Model (2). The M5 Method
400 was used as attribute selection method for the linear model presented.
401
402
403
404

405
406 Two models were produced to achieve the objectives of our work:
407
408
409
410
411
412
413

- 414
415
416
417
418
419
420
421
422
423
424
425
426
427
- Model (1) is based on a classic decision tree model, developed to be used in the field in order to predict a B_d class using only visual descriptors as in Table 1.
 - Model (2) is a linear regression model that uses the same in-field descriptors as above, and it is able to predict a numerical value of B_d with a relatively small error.

428
429
430
431
432
433
434
435
436
437
438
439
440

The proposed two models are both descriptive and predictive, but the decision tree is better at exploring in a descriptive way the relationship between B_d and visual parameters, as it allows further analysis of the soil pertaining to that soils own chemical and physical characteristics. On the other hand, the linear equation algorithm is stronger as a predictive tool and it offers a more precise estimate of B_d .

441 **2.3.1 Data treatment**

442
443
444
445
446
447

The entire database consists in 201 sampling points (profile pits) for a total of 471 horizons. For each horizon eleven descriptors and B_d data were used to train Model (1) and Model (2). The treatment of data can be summarized as follows:

- 448
449
450
451
452
453
454
455
456
457
458
459
460
461
462
463
464
465
466
467
468
469
470
471
472
- Data cleaning: to produce a full dataset, time was invested to ensure the data homogeneity between Irish SIS (649 horizons) and SQUARE datasets (125 horizons). In particular, descriptor rating options were double checked to reaffirm consistency across projects. To achieve uniformity within the dataset some data conversions were necessary. The final dataset consisted of 471 horizons i.e. 346 from Irish SIS and 125 from SQUARE.
 - Missing values imputation: an initial analysis of the dataset highlighted the presence of some missing values for part of the considered descriptors, namely: “Fissure size”, “Void size”, “Void abundance” and “Soil consistency”. To avoid further reductions of the dataset, an IMRI imputation (performed by the WEKA 3.8 software described above) was selected as the means to predict missing values (Templ et al., 2011).

2.3.2 Model 1: Decision tree model, validation and outputs

Model (1) has been designed to predict classes of B_d data through the combination of the 11 visual descriptors outlined in Table 1. The model has been trained using B_d data at horizon level. The predicted classes of B_d are:

- (i) Low B_d class: $< 1.0 \text{ g cm}^{-3}$ (n=137 cases)
- (ii) Medium B_d class: between 1.0 and 1.4 g cm^{-3} (n=178 cases)
- (iii) High B_d class: $> 1.4 \text{ g cm}^{-3}$ (n=156 cases)

Class ranges were selected on the basis of their homogeneity in terms of class population. The B_d measured in the majority of mineral soils under agricultural management in Ireland occur typically within the 1.0 and 1.4 g cm^{-3} range. Values of $< 1.0 \text{ g cm}^{-3}$ are usually related to Ombrotrophic or Mineratrophic Peat Soils (which correlates with the Histosol reference soil group of the WRB (IUSS Working Group WRB, 2006) or mineral soils having a Histic horizon (Reidy et al., 2016). Therefore 1.0 g cm^{-3} was selected as the lower B_d threshold e.g. herein 16 cases out of 137 belonged to the Low B_d class as Oh, Op, Of or Omf. The higher threshold (1.4 g cm^{-3}) was empirically chosen to best fit these data. In particular, multiple decision tree models were trained by varying the threshold between 1.1 g cm^{-3} and 1.8 g cm^{-3} , in 0.1 intervals. The model trained with the 1.4 g cm^{-3} threshold outperformed, other model runs in terms of accuracy.

The decision tree produced herein can be easily converted into classification rules. Each path in the tree that goes from the root to one of the leaves defines one classification rule. In our case each rule categorises the data in B_d Low, Medium and High classes. The knowledge represented in a decision tree can be extracted and represented in the form of the classification rule IF-THEN as follows:

532
533
534 **If** {condition A} AND {condition B} AND {condition C} AND {...} **then**
535 categorization.
536
537
538

539
540 In our case:

541
542 **If**

543 the horizon is described as HUMOSE

544
545
546 **then**

547 the horizon fits into the bulk density category “Low”= $<1 \text{ g cm}^{-3}$
548
549
550

551 A pruning technique is automatically performed by the WEKA software. This
552 allows the identification and the removal of the outliers reducing the risk of
553 overfitting to the training data (Bhargava et al., 2013). When decision trees are
554 built, many of the ramifications can represent noise or outliers in the training
555 data. The pruning process tries to identify and remove these branches with the
556 aim of improving the accuracy of classification of future data. The next step was
557 to prune the dataset to identify and remove branches which do not improve
558 prediction with the aim of improving the accuracy of classification of future
559 data. The pruning process tries to identify and remove these branches with the
560 aim of improving the accuracy of classification of future data. The next step was
561 to prune the dataset to identify and remove branches which do not improve
562 prediction with the aim of improving the accuracy of classification of future
563 data. The pruning process tries to identify and remove these branches with the
564 aim of improving the accuracy of classification of future data. The next step was
565 to prune the dataset to identify and remove branches which do not improve
566 prediction with the aim of improving the accuracy of classification of future
567 data.
568

569 A10-fold cross validation method was adopted, which randomly partitions the
570 dataset into 10 parts and is used to validate the model. Then nine parts of the
571 dataset were used to train the model, with the last part used for model testing
572 (see Xue et al., 2015 for a similar approach).
573
574
575
576
577

578
579 Two measures were applied to evaluate the model performance; precision and
580 recall values were calculated. Precision indicates how many of the instances
581 were classified within a certain class that actually belong to that class. Whereas
582 recall indicates how many of the instances that belong to a certain class are
583
584
585
586
587
588
589
590

591
592
593
594 correctly classified by the model. To explain these measures further, it is useful
595 to introduce the concepts of true positive, false positive and false negative.

597 Given a class C , we define true positives tp as the number of instances labelled
598 as C in the original dataset, and classified as C by the decision tree; false
599 positives fp as the number of instances not labelled as C in the original dataset,
600 and incorrectly classified as C by the decision tree; false negatives fn as the
601 number of instances labelled as C in the original dataset, and not classified as C
602 by the decision tree. Given these definitions, precision p_C and recall r_C for the
603 class C are defined as follows:
604
605
606
607
608
609

$$610 \quad p_C = \frac{tp}{tp + fp}; \quad \text{Eq 2}$$

$$611 \quad r_C = \frac{tp}{tp + fn} \quad \text{Eq 3}$$

612
613
614
615
616
617 Precision is negatively influenced by the number of false positive cases.
618 Whereas, recall is negatively influenced by the number of false negative cases.
619 High scores for precision and recall show that the classifier is returning accurate
620 results (high precision, related to low false positive rates), as well as returning a
621 majority of all positive results (high recall, related to a low false negative rates).
622
623
624
625
626

627
628 As no baseline algorithms were available, or proposed in other publications,
629 against which to evaluate the performance of our Model (1), we resort to
630 comparing it with a random predictor baseline, i.e. a fictional algorithm that
631 randomly predicts the class of an instance (Alvarez, 2002).
632
633

634
635 Let n be the total number of instances, and let c be the number of instances of
636 class C , the precision and recall of a random predictor for the class C is given
637 by:
638
639

$$640 \quad p_C = r_C = c / n \quad \text{Eq 4}$$

Besides precision and recall for each class, we also evaluated the average value of these measures. In addition, we evaluated the harmonic means of precision and recall, which is normally called F-measure, and is defined as follows:

$$F\text{-measure} = 2 * \frac{p_c * r_c}{p_c + r_c} \quad \text{Eq 5}$$

Finally, as an overall indicator of the ability of the decision tree to correctly classify the instances, we evaluated the overall accuracy, which is defined as follows:

$$Accuracy (\%) = \frac{tp + tn}{tp + tn + fp + fn} \quad \text{Eq 6}$$

2.3.3 Model 2: Linear regression model, validation and outputs

Using data from the visual parameters (Table 1), a linear equation that predicted an exact B_d value was developed.

As for Model (1), Model (2) was learned using B_d data at horizon level and produced by means of the WEKA software, using a linear regression algorithm. For this experiment these data were converted into numerical binary data, since the linear regression algorithm takes numerical data as input. In particular, for each value taken by each descriptor, a binary variable was created that takes either 0 (False) or 1 (True) as values. The variable was 1 if the descriptor had the value associated to the variable, and 0 otherwise.

The model builds a linear equation based on a weighted combination of the possible values taken by the 11 descriptors. In particular, the linear model has the following form:

$$B_d (g\ cm^{-3}) = \sum_{i=0}^n C_i * V_i \quad \text{Eq 7}$$

where C_i are the coefficients computed by the linear regression algorithm. V_i are the binary variables. The linear regression algorithm is designed to select only those variables that have an influence on the final B_d value. Hence, the final model will not include all the possible variables, but only a subset. A 10-fold cross validation was performed to validate the model as described in par 2.3.2.

For Model (2) we could not evaluate the performance through precision and recall, since numerical values are involved instead of categorical ones, but we evaluated it in terms of correlation coefficient, root mean squared error, and mean absolute error:

The Root Mean Squared Error (RMSE) gives an estimation of the standard deviation of the error (Henderson et al., 2005). The lower is RMSE the higher is the predictive ability. Where n is the size of the dataset and \hat{y}_t is the predicted value, the formula is defined as follows:

$$RMSE = \sqrt{\frac{1}{n} \sum_{t=1}^n (y_t - \hat{y}_t)^2} \quad \text{Eq 8}$$

The Mean Absolute Error (MAE) is a quantity used to measure how close predictions are to the eventual outcomes. The mean absolute error is also known as the mean absolute deviation (Henderson et al., 2005). The lower the MAE value the higher is the predictive ability.

$$MAE = \frac{1}{n} \sum_{t=1}^n |y_t - \hat{y}_t| \quad \text{Eq 9}$$

3. Results and discussion

3.1 Model 1: Decision tree approach to assess B_d classes

3.1.1 Model performances

The number of rules generated by the decision tree algorithm was 41 in total; 11, 13 and 17 for Low, Medium and High respectively (all the rules are reported in Table 2 in the Supplementary Material). The overall tree is reported in Figure 1. The decision tree hierarchy consists of six levels (level 1 has the highest classification power) of depth as follows:

Level (1): Humose

Level (2): Structure type

Level (3): Macropores Size/Void Size/Void Abundance/Plasticity

Level (4): Structure Grade/Stickness

Level (5): Fissures

Level (6): Structure size

The descriptor “soil consistency” was excluded by the tree hierarchy, showing no influence on the prediction of B_d ranges. To discuss these results, it is useful to associate the different levels and hence, the corresponding descriptors, to specific soil quality properties. Broadly the descriptors that remained in the analysis fell into 4 main groups in order of importance as follows:

(i) soil humic characteristics; explained by level (1);

(ii) pedogenic formation; explained by level (2);

(iii) soil porosity; explained by level (3);

(iv) soil cohesive properties; explained by level (3-4).

The majority of the 41 rules were classified within the first three hierarchical levels highlighting the importance of these soil structural descriptors in quantifying B_d class. In general the parallelism between soil aggregation mechanisms, soil intrinsic characteristics related to soil forming factors, and the

827
828
829 arrangement of solid and voids with their capacity to retain and transmit fluids,
830
831 resulted in the main factors being capable of explaining soil B_d .
832
833
834

835 The overall accuracy shows that the model correctly classified 71% of the
836 training data (Table 2). However, after the 10-fold cross validation step the
837 model was able to correctly predict 60% of the cases (Table 2). The confusion
838 matrix shows that mis-categorisation does not occur from Low to High B_d
839 classes and vice versa, but can occur from Low to Medium (46 cases) and from
840 High to medium (52 cases) (Table 3). The cause of lower model performance
841 can be clarified by looking at the branches of the decision tree that miss-classify
842 the highest number of instances (for discussion see par. 3.2.1).
843
844
845
846
847
848
849
850

851 The decision tree model was evaluated using the random predictor method (see
852 par. 2.3.2). Performances are the following:
853
854

855 Low: $p_L = r_L = 137/471 = 0.29$.

856 Medium: $p_M = r_M = 178/471 = 0.37$.

857 High: $p_H = r_H = 156/471 = 0.33$.
858
859
860
861
862

863 For the Low B_d class, the decision tree outperforms a random predictor by 40%
864 in terms of precision and by 25% in terms of recall; for the Medium B_d class, by
865 16% in terms of precision and by 26% in terms of recall; for the High B_d class
866 by 30% in terms of precision and by 29% in terms of recall. These figures
867 indicate that, although the accuracy indicates poor performance for the Low B_d
868 class, the prediction for this class in terms of precision is actually the best
869 amongst all 3 classes. This is due to the lower number of Low B_d instances,
870 which are harder to detect for a random classifier, and that our algorithm
871 predicts with a substantially higher degree of precision. Overall, the
872 classification produced by the model is considerably better than a random
873 classification.
874
875
876
877
878
879
880
881
882
883
884
885

3.1.2 Rules analysis

Figure 1 shows the decision tree generated for each B_d class with the corresponding instances classified for each rule and the percentage of accuracy, which refers to the percentage of true positive cases found by the model for the rule discussed. Rules classifying less than two instances are not reported in these figures.

- **Level 1: “Humose”**

The “**Humose**” descriptor emerges as the most dominant discriminator. All the horizons that highlight the presence of the “humose” feature following the rule “Humose: *yes*”, fit in the category Low B_d . The model correctly classifies 85.9% of $n=64$ instances for this rule with relatively few false positive cases.

The humose feature refers to an estimation of the level of humification of the organic material, so it is indirectly related to the C content. In fact, soil OC content gives an indication of decomposition rates which have a direct effect on soil aggregation (Bronick and Lal, 2005; Schulten and Leinweber, 2000). The presence of humic substances, as well decomposed organic matter (OM), contributes to the stability of soil aggregates and pores through the bonding or adhesion properties of organic materials, such as bacterial waste products, organic gels, fungal hyphae and worm secretions and casts. Moreover, OM intimately mixed with mineral soil materials induces increased moisture holding capacity and air exchange with the atmosphere (Stevenson, 1994). This mechanism is reflected by lower values of B_d , resulting in enhancement of soil porosity producing a good soil structure.

When the humose feature is recorded as absent, the model switches to level 2 for further refinement.

945
946
947
948
949
950
951
952
953
954
955
956

- **Level 2: “Structure Type”: Granular**

957
958
959
960
961
962
963
964
965
966
967
968
969
970
971
972
973
974
975
976
977
978
979
980
981
982

“Structure Type” was the most discriminating descriptor at the second level of the tree hierarchy. Here the tree branches out to account for the effect of different types of structure.

983
984
985
986
987
988
989
990
991
992
993
994
995
996
997
998
999
1000
1001
1002
1003

For the rule “Humose: *no*, AND Structure type: *Granular*” the model classified 23 cases as belonging to the Low B_d class, with an accuracy of 56.5%. Despite the high number of false positives, the amplitude of the group is among the highest, showing its reliability.

Granular aggregates are spheroids or polyhedrons aggregates of soil, having curved or irregular surfaces (FAO, 2006), they are normally associated with highest air capacity, and are an indicator of good soil structure (Mueller et al., 2009). Such cases are mostly A horizons, not deeper than 30 cm. Root mass, density, distribution and turnover, can positively influence the soil particle aggregation by releasing a variety of compounds, (such as root exudates) and can contribute to increased soil porosity through mechanical action (Bronick and Lal, 2005; Caravaca et al., 2002). This is reflected in the B_d, resulting in lower values.

- **Level 2: “Structure Type”: Subangular Blocky → Level 3, “Macropores Size” → Level 4 “Structure Grade”**

In presence of the “Subangular Blocky” structure type the tree branches split again, going deeper into the third hierarchical level of tree structure, showing the “Macropores size” descriptor as the next level of description. For the rules “Humose: *no*, AND Structure type: *Subangular Blocky* AND Macropores: (*A*), (*B*), (*C*), (*D*)”:

(*A*) Coarse (C 5.0-20.0 mm): 50% accuracy when classifying Low B_d class.

(*B*) Fine (F 0.5-2.0 mm): for subangular blocky aggregates, 66.1% accuracy when classifying Medium B_d class. This is a rule that has a higher number of

1004
1005
1006 instances (n=92), which balances the presence of a relatively high number of
1007 false positives. For angular blocky aggregates, 72.7% accuracy when classifying
1008 Medium B_d class (n=11).
1009

1010 (C) Very Fine (VF < 0.5 mm): 66.7% accuracy when classifying High B_d class.
1011

1012 (D) Medium (M 2.0-5.0 mm): 100% accuracy when classifying Low and
1013 Medium B_d class.
1014
1015

1016 Subangular blocky structure type is described as cube like with a flat surface
1017 and rounded corners (FAO, 2006; Schoeneberger et al., 2012) and is considered
1018 an indicator of an intermediate degree of soils structure quality, between the
1019 granular/crumblly aggregates and the blocky/sharp angular ones. Results for this
1020 structure type show that the size of the macropores is a crucial variable to
1021 discriminate in terms of B_d classes, as B_d is very sensitive to both alteration of
1022 macroporosity abundance and size of pores (Mueller et al., 2009). In particular
1023 the higher the macropore size, the lower the B_d class predicted by the model.
1024
1025
1026
1027
1028
1029
1030
1031
1032
1033

1034 For the rule (A), horizons fitting the Low B_d class are mostly Ap horizons,
1035 corresponding to the upper soil layers (maximum depth of 22 cm). Earthworm
1036 activity is mainly concentrated in the top soil (Haynes and Naidu, 1998; Lee and
1037 Foster, 1991), which promotes macropores (C 5.0-20.0 mm) which in turn can
1038 alter soil porosity thereby affecting the movement of air, water and solutes
1039 (Shipitalo and Le Bayon, 2004). For the rule (B) and (C) medium and high B_d
1040 are associated with macropore sizes from 0.5 mm to 2.0 mm. The cases
1041 following these two rules are mainly classified as A or B horizons for the
1042 medium B_d class (average maximum depth of ~40 cm) and as B horizons for the
1043 higher B_d class (average maximum depth of ~60 cm). At such depths roots
1044 become thinner resulting in reduced porosity and higher B_d. Furthermore, B_d
1045 often increases in the deeper horizons due to an increase in clay material or as
1046 result of management operations.
1047
1048
1049
1050
1051
1052
1053
1054
1055
1056
1057
1058
1059
1060
1061
1062

1063
1064
1065
1066
1067
1068
1069
1070
1071
1072
1073
1074
The medium class of macropores (M 2.0-5.0 mm) insufficiently defines the B_d range and must be assisted by another splitting attribute which is triggered at level four. The “**Structure grade**” is identified by the model as an important variable to discriminate between the Low and Medium B_d class for this macropores size. The rule (*D*) is consequently developed as follows:

- 1075 • “Humose: *no*, AND Structure type: *Subangular Blocky* AND Macropores: *M*
1076 *2.0-5.0 mm* AND Structure grade: *Moderate*”; which predict Low B_d class
1077 (100% correct instances).
1078
- 1080 • “Humose: *no*, AND Structure type: *Subangular Blocky* AND Macropores:
1081 *M 2.0-5.0 mm* AND Structure grade: *Weak*”; which predict Medium B_d class
1082 (100% correct instances).
1083
1084
1085

1086
1087
1088
1089
1090
1091
1092
1093
1094
1095
1096
1097
1098
1099
1100
1101
1102
1103
1104
1105
1106
1107
1108
1109
1110
1111
1112
1113
1114
1115
1116
1117
1118
1119
1120
1121
FAO (2006) defines soils by describing the lack (apedal) or the presence (pedal) of a defined structure. A moderate structure grade, showing the presence of a nicely structured soil, was associated with a Low B_d class. Medium B_d classes are associated with a weak structure grade, synonymous of a lower structure quality. However, herein cases classified for these two rules were similar in terms of actual B_d values. In particular, cases classified as Low B_d had actual values very close to the upper limit of this category (values between 0.9 and 1.0 g cm⁻³) and the cases classified as Medium B_d had actual values close to the lower limit of this category (values between 1.0 and 1.16 g cm⁻³). Considering the narrow range of values for these cases across the Low and Medium B_d categories the model correctly discriminates between categories.

- **Level 2: “Structure Type”: Angular Blocky → Level 3, “Void Size” → Level 4 ”Stickiness”**

The “Angular Blocky” aggregates belong to the blocky category as for the subangular blocky aggregates, but differ as they have faces intersecting at relatively sharp angles (FAO, 2006; Schoeneberger et al., 2012). In the presence of this structure type i.e. a typical indicator of a poorly structured soil, the

1122
1123
1124 model returns “**Void size**” as the next, most important, descriptor. This
1125 descriptor indicates the total volume of pores discernible with a *10 hand-lens
1126 (FAO, 2006). It differs from macroporosity as it is a much wider term that
1127 includes soil fissures and plane (FAO, 2006). Macropores are mostly
1128 determined by plant roots through the twisting activity within and around
1129 aggregates, and by zoological exploration, through burrowing activity, so they
1130 are usually larger pores having a size higher than 75 μm (Russell, 1975).
1131 However, here macropores and voids are described in terms of size, so a high
1132 void size can correspond to a high macropores size. Therefore, it is important to
1133 highlight here that although different from a semantic point of view, the
1134 combination of these two descriptors was very effective in explaining soil
1135 porosity.
1136
1137
1138
1139
1140
1141
1142
1143
1144
1145
1146
1147

1148 For the rule “Humose: *no*, AND Structure type: *Angular Blocky* AND Void
1149 size: *C 5.0-20.0 mm*” the model returned 75% of correct instances for the class
1150 Low B_d . Although the structure type indicated was often that of a very poor
1151 structured soil, characterised by large, angular and sharp aggregates, this effect
1152 was mitigated by the presence of a very high overall porosity, resulting in a
1153 Low B_d (Pagliai and Vignozzi, 2002).
1154
1155
1156
1157
1158
1159

1160 The rule “Humose: *no*, AND Structure type: *Angular Blocky* AND Void size:
1161 *VF < 0.5 mm*”, returned High B_d class with 76.9 % accuracy. Also this rule was
1162 quite wide in terms of population (n=26). In this case the poorly structured
1163 horizons were associated with the smallest size of pores. The cases are mainly
1164 classified as Bg, BCg, Cg or Eg horizons, with an average depth ranging from
1165 42 to 72 cm. For such cases, gleying is caused by surface water which has been
1166 held in a poorly permeable horizon, (mainly belonging to surface water gley soil
1167 type (Stagnosols reference soil group of the WRB). These poorly permeable
1168 layers showed evidence of compaction due to one or more of the following
1169 characteristics: (i) presence of a pan, resulting in severe compaction imposed by
1170
1171
1172
1173
1174
1175
1176
1177
1178
1179
1180

1181
1182
1183 management, (ii) poor structural development, (iii) very heavy textured
1184 horizons dominated by silt and clay and (iv) natural impeded horizons due to
1185 soil formation and profile development mechanisms.
1186
1187

1188
1189 Furthermore, the presence of some argillic horizons classified as Btg following
1190 this rule, as well as having gleyic features, showed the presence of clay-sized
1191 material in coatings or as intrapedal concentrations (FAO, 2006). Clay content
1192 physically affects particle aggregation through swelling and dispersion,
1193 resulting in contiguous peds which fit together eliminating space (Attou et al.,
1194 1998; Bronick et Lal, 2005; Kay, 1998; Russel, 1975).
1195
1196
1197
1198
1199
1200
1201

1202 When the void size is classified as belonging to the middle category (Humose:
1203 *no*, AND Structure type: *Angular Blocky* AND Void size: *F 0.5-2.0 mm*),
1204 “**Stickiness**” was selected by the model as the next most informative descriptor,
1205 associating Medium B_d class with the “*Non Sticky OR Slightly Sticky*” feature
1206 (50% and 63.6% accuracy, respectively), and the High B_d class with the
1207 “*Sticky*” feature (accuracy of 75%). The rules’ population size was n=44, n=22
1208 and n=12, respectively and therefore must be considered an important branch of
1209 the overall tree. As the stickiness property is considered an indirect indicator of
1210 the clay content in soil, the results confirmed that the presence of clay material
1211 was one of the characteristics which makes the soil prone to compaction, or at
1212 least significantly decreases the level of porosity. Even in the presence of a
1213 relatively higher porosity, clay content was crucial to force a split in B_d classes,
1214 thereby attributing higher B_d values to heavier textured soils.
1215
1216
1217
1218
1219
1220
1221
1222
1223
1224
1225
1226
1227

1228 “**Plasticity**” appears at the third depth level of the decision tree for the
1229 structure type Angular Blocky to Granular. Like stickiness, plasticity is directly
1230 related to the clay content (FAO, 2006). Horizons classified as “*Plastic OR*
1231 *Slightly plastic* AND Macropores size: *Very Fine (VF < 0.5 mm)*”, fit into the
1232
1233
1234
1235
1236
1237
1238
1239

1240
1241
1242 High B_d class, highlighting the link between high values of B_d and clay content
1243 (accuracy respectively of 100% and 66.7%).
1244
1245
1246
1247

- **Level 2: “Structure Type”: Prismatic → Level 3, “Void Abundance”
→ Level 4 ”Structure Grade” → Level 5: “Fissures”→ Level 6:
“Structure Size”**

1248
1249
1250
1251
1252
1253
1254 The “Prismatic” structure type is described by FAO, (2006) and by
1255 Schoeneberger et al. (2012) as having vertical elongated units with limited faces
1256 in the horizontal plane. Horizons having prismatic to angular blocky aggregates
1257 are classified by the model within the High B_d class (accuracy, 62.5%). The
1258 average depth ranges within 53-95 cm, classified across a number of soil types
1259 e.g. typical surface water gleys (Stagnosols reference soil group of the WRB),
1260 typical luvisols (Luvisols), typical brown podzolic (Podzols) and typical
1261 calcareous brown earths (Calcaric Cambisols). Different soil types are subjected
1262 to different mechanisms of soil particle aggregation which can exert a degree of
1263 compaction in a specific horizon, due to their intrinsic nature or to a
1264 combination of factors, such as: (i) clay concentrations in the impeded horizon,
1265 as for luvisols; (ii) translocation of Al and Fe in the spodic horizon, as for
1266 brown podzolic (Bronick and Lal, 2005; Collins, 2004), (iii) presence of
1267 carbonates, as for the calcareous brown earths (Boix-Fayos, et al., 2001) and
1268 (iv) presence of a poorly permeable horizon, as for the gleyic horizons in
1269 surface water gleys (Collins et al., 2004).
1270
1271
1272
1273
1274
1275
1276
1277
1278
1279
1280
1281
1282

1283 Furthermore, for the prismatic structure type, “**Voids abundance**” is selected as
1284 the main descriptor to split the data between High and Medium B_d for this
1285 structure type.
1286
1287
1288

1289 For the rules “Humose: *no*, AND Structure type: *Prismatic* AND Void
1290 abundance: *A, B, C*:

1291 (*A*) High (15-40%): the model returns 66.7% of correctly classified instances as
1292 belonging to the Medium B_d class,
1293
1294
1295
1296
1297
1298

1299
1300
1301
1302 (B) Very Low (<2%): the model classifies for the High B_d class with an
1303 accuracy of 75%.
1304

1305 (C) Medium (5-15%): the model classifies for Medium and High B_d with an
1306 accuracy of 83.3 and 89%, respectively.
1307
1308

1309 The Low B_d category was not defined by the model for this structure type,
1310 indicating the prismatic arrangement as having overall higher B_d values. The
1311 abundance of voids is important, as the void size for this type of structure,
1312 poorer than the angular blocky structure type. Rules (A) and (B) associated
1313 higher void abundance with higher structure quality. On the other hand the rule
1314 (C), which took into account the medium void abundance category, requires
1315 further descriptors to categorise within the High and the Medium B_d classes,
1316 such as “**Structure grade**”, “**Fissures**” and “**Structure size**”.
1317
1318
1319
1320
1321
1322

1323 The presence of smaller sized prismatic aggregates (Structure size: *Fine 10-20*
1324 *mm*) directs the model to predict High B_d class with 100% correct instances. As
1325 found in the present study, the rapid wetting of dry soil which comes in contact
1326 with free water can cause micro-cracking. This increases ped friability, causing
1327 the production of smaller sized aggregates, which does not always result in
1328 lower values of B_d (Dexter, 2002).
1329
1330
1331
1332
1333
1334
1335
1336

1337 Vertical fissures are also an important feature of this structure type. Although
1338 hard clods are devoid of microstructure, fissures enable the percolation of the
1339 surface water in the deeper layers (Russel et al., 1975). Such a drainage
1340 advantage is not valid for the “Platy” structure type. In this case the model
1341 returns two different outputs. Platy aggregates, probably formed by intensive
1342 mechanical intervention, indicate compaction which affects water percolation,
1343 resulting in high B_d values (accuracy, 66.7%). On the other hand, some platy
1344 aggregates were attributed to the histic horizons (Of, Omf) which showed no
1345 developed structure, associated with very low B_d (accuracy 75%).
1346
1347
1348
1349
1350
1351
1352
1353
1354
1355
1356
1357

1358
1359
1360
1361 • **Level 2: “Structure Type”: Massive**

1362 Structure types defined as “Massive” and “Single grain” were categorised by
1363 Schoeneberger et al. (2012) as structure less soils. Massive soil material
1364 normally has stronger consistence as the soil particles are arranged in a coherent
1365 mass and are very difficult to break (FAO, 2006). Horizons with “Massive”,
1366 “Massive to Angular blocky” and “Massive to Single Grain” structure types
1367 were classified by the model as belonging to the High B_d class with an accuracy
1368 of 77.8%, (n=63; very influential rule in the overall tree output), 83.4% and
1369 100%, respectively. Further analysis of the data showed that most of the
1370 horizons belonging to the rule: “Humose: *no*, AND Structure type: *Massive*”
1371 were described as having a hard or very hard consistence dry, fine or very fine
1372 macropores and very low void abundance. The decrease in soil macroporosity
1373 and the firm nature of the aggregates suggests a high level of compaction
1374 (Epron et al., 2016), resulting in high B_d values which ranged from 1.4 g cm⁻³ to
1375 1.9 g cm⁻³. In the case of the Massive to single grain structure type, “**Plasticity**”
1376 is a key attribute to assess the range of B_d (rule: “Humose: *no*, AND Structure
1377 type: *Massive to Single grain* AND Plasticity: *Non plastic*”).
1378

1379 The arrangement of the aggregates which are weak and tend to disintegrate
1380 when sampling in the field, suggested the presence of sandy material held
1381 together in big, hard and massive aggregates. In some soils, sand grains have a
1382 film of orientated clay particles on the surface, not enough to be detected by
1383 feel, but that are able to strongly hold the sand particles packing them together
1384 in massive aggregates (Russel, 1975). Sandy soils are prone to compaction of
1385 surface layers, due to intensive agricultural operations (Ampoorter et al., 2007;
1386 Deconchat, 2001; Teepe et al., 2004).
1387

1388 Low B_d class was attributed by the model to the horizons responding to the rule
1389 “Humose: *no*, AND Structure type: *Single grain*”, which is a feature typical of
1390 sandy soils not subjected to compaction phenomena, thereby conserving a large
1391
1392
1393
1394
1395
1396
1397
1398
1399
1400
1401
1402
1403
1404
1405
1406
1407
1408
1409
1410
1411
1412
1413
1414
1415
1416

1417
1418
1419 amount of wide pores (Ampoorter et al., 2007). The model correctly classified
1420 66.7% of the instances following this rule.
1421
1422
1423
1424

1425 **3.2 Model 2: Linear regression approach to predict a numerical estimate of** 1426 **B_d** 1427

1430 **3.2.1 Model and performance** 1431

1432 After several trials with different machine learning methods for numerical
1433 prediction, a linear regression model was selected based on better overall
1434 performance. This conclusion asserts that a strong linear relationship exists
1435 between the visual descriptors and B_d values. As a result, since the model
1436 produced by a linear regression algorithm is a linear equation, the predicted
1437 value of B_d can be easily computed in seconds without the need for time
1438 consuming and costly laboratory analyses.
1439
1440
1441
1442
1443
1444
1445
1446

1447 Model (2) considers only those descriptors that influence the final B_d value. For
1448 this quantitative estimation seven descriptors out of eleven were selected by the
1449 linear regression algorithm:
1450
1451
1452

- 1453 (i) Humose
 - 1454 (ii) Structure Grade
 - 1455 (iii) Structure Type
 - 1456 (iv) Structure Size
 - 1457 (v) Macropores
 - 1458 (vi) Void Size
 - 1459 (vii) Void Abundance
- 1460
1461
1462
1463
1464
1465
1466
1467
1468
1469
1470
1471
1472
1473
1474
1475

The linear equation produced by Model 2 to predict B_d is as follows:

$$\begin{aligned} B_d \text{ (g cm}^{-3}\text{)} = & \\ & 0.4575 * (\text{NO Humose: =true}) + \\ & -0.0517 * (\text{MODERATE Structure Grade=true}) + \\ & -0.2128 * (\text{GRANULAR Structure Type=true}) + \\ & 0.093 * (\text{MASSIVE Structure Type=true}) + \\ & -0.134 * (\text{SUBANGULAR BLOCKY Structure Type=true}) + \\ & -0.1501 * (\text{SUBANGULAR BLOCKY TO GRANULAR Structure Type=true}) + \\ & -0.1003 * (\text{ANGULAR BLOCKY TO GRANULAR Structure Type=true}) + \\ & -1.1619 * (\text{VERY COARSE > 10mm Structure Size=true}) + \\ & 0.1471 * (\text{VERY FINE < 0.5mm Macropores=true}) + \\ & -0.1791 * (\text{COARSE 5-20 mm Void Size=true}) + \\ & 0.0802 * (\text{VERY LOW Void Abundance=true}) + \\ & -0.0784 * (\text{HIGH Void Abundance=true}) + \\ & 0.8866 \end{aligned} \tag{Eq 10}$$

The equation produced follows a simple framework:

(i) All the descriptors associated with a *positive coefficient* caused a significant incremental increase in B_d . Basically, as the associated coefficients are positive, a soil classified having these descriptors ($V_i=1=true$, see description in paragraph 2.3.3), will result in an increased B_d final value.

The variables “*NOHumose=true*”, “*VERY FINE<0.5mm Macropores=true*”, “*VERY LOW Void Abundance=true*” and “*MASSIVE Structure Type=true*”, all cause an increase in B_d , with 0.4575; 0.1471; 0.0802; and 0.093 explanatory power, respectively.

1535
1536
1537
1538 In line with Model (1) results, the humification degree of OM has the greatest
1539 influence on B_d prediction. This characteristic, as well as readily defining B_d
1540 class, also informed small differences in soil B_d and generally indicated
1541 pedological features that were consistent with lower B_d values.
1542

1543
1544 Following the humic feature, macropores size was the second more
1545 discriminating feature, with the lower size able to distinguish a wide increment
1546 of prediction (multiplier of 0.1471). Furthermore, very low void abundance
1547 triggered the model as the fourth main attribute (multiplier of 0.0802). This was
1548 an expected result, as porosity was already investigated by the decision tree
1549 approach and was one of the most critical soil characteristics which took into
1550 account an evaluation of soil structure. In particular, size of pores was
1551 highlighted as a stronger predictor for an increase of B_d with respect to pore
1552 abundance. As seen from the decision tree output, the massive structure type has
1553 a role in increasing soil B_d . In general both models although operating at
1554 different scales produce the same descriptors for the prediction of B_d .
1555
1556
1557
1558
1559
1560
1561
1562
1563
1564
1565
1566

1567 (ii) All the descriptors associated with a *negative coefficient* have a role
1568 decreasing B_d . Basically, as the associated coefficients are negative, a soil
1569 classified as having these descriptors, resulted in a decreased B_d , and therefore
1570 have a better soil physical quality.
1571
1572
1573
1574
1575

1576 In Model (2), structure size appears to be a stronger descriptor which influences
1577 a decrease in B_d when evaluated as “*VERY COARSE > 10 mm Structure*
1578 *Size=true*” (multiplier of -1.1619). This was surprising considering that in
1579 Model (1) the size of aggregates was not particularly important (sixth level) in
1580 the tree hierarchy as a splitting attribute. This highlights that this feature is
1581 better at identifying small incremental reductions of B_d , but is less informative
1582 when splitting into wider B_d ranges.
1583
1584
1585
1586
1587
1588
1589
1590
1591
1592
1593

1594
1595
1596
1597 However, in Model (2) Structure type still has to be considered one of the most
1598 informative variables, since it appears in four out of eight factors having a
1599 negative coefficient in the equation. In particular, looking at the equation, we
1600 have:
1601
1602

- 1603 • “*GRANULAR Structure Type=true*” ,
- 1604 • “*SUBANGULAR BLOCKY TO GRANULAR Structure Type=true*” ,
- 1605 • “*SUBANGULAR BLOCKY Structure Type=true*” ,
- 1606 • “*ANGULAR BLOCKY TO GRANULAR Structure Type=true*” ,
- 1607
- 1608
- 1609

1610 as coefficients -0.2128; -0.1501; -0.134; -0.1003, respectively.
1611

1612 Granular structure type is responsible of a higher decrease of B_d , confirming
1613 what was found for Model (1), indicating good soil structure.
1614
1615
1616

1617
1618 The model showed sufficient sensitivity allowing the identification of
1619 differences related to soil structure type. This is despite the relatively crude
1620 measurement of soil structure at field level in tandem with other attributes. In
1621 particular while the soil structure quality, associated with a change of structure
1622 type, gradually decreases, with diminishing negative effect on B_d , indicated by
1623 the coefficients for individual structure types. Hence, corresponding to their
1624 respective coefficients, a granular structure type will have a higher negative
1625 increment, resulting in a reduction of the B_d final value, while an angular blocky
1626 to granular structure type will have a lower negative reduction in the final
1627 predicted value, resulting in a higher B_d final value.
1628
1629
1630
1631
1632
1633
1634
1635
1636

1637
1638 Structure size, Void size, Void abundance and Structure grade were, in order of
1639 importance, the next most informative features for the linear regression model.
1640

1641 If both the features relating to porosity appear in the Model (1) at a high level in
1642 the tree hierarchy (level 3), for this model only void size with the variable
1643 “*COARSE 5-20 mm Void Size=true*” appears to have higher negative impact,
1644 with a relatively high coefficient of -0.1791, while void abundance (*HIGH Void*
1645
1646
1647
1648
1649
1650
1651
1652

1653
1654
1655
1656 *Abundance=true*) resulted in having less negative impact on the definition of a
1657 final B_d value, being associated with a smaller coefficient, -0.0784. Probably, as
1658 per the decision tree model, the shape of aggregates is again a critical point
1659 which drives the selection of the second decisive node into pore abundance or
1660 size, depending on the original structure type.
1661
1662
1663
1664
1665
1666

1667 **3.2.2 Overall model evaluation**

1668
1669 The overall correlation coefficient on training set for the linear regression model
1670 is 0.71 with Root Mean Squared Error (RMSE): 0.25 and Mean Absolute Error
1671 (MAE): 0.20; (Table 4). After a 10-fold cross validation the correlation
1672 coefficient slightly dropped, to 0.65, with similar error ranges (RMSE: 0.27 and
1673 MAE: 0.21); (Table 4). The errors reported for this model may be considered
1674 quite high in relation to a standard lab-based B_d measure. However, it is
1675 important to highlight that the model has been fed using only soil visual
1676 parameters. Considering the nature of these data inputs and the influence that
1677 different operators can have during the classification phase, this range of error is
1678 low.
1679
1680
1681
1682
1683
1684
1685
1686

1687 Figure 2 shows the prediction performances of Model (2). The distribution of
1688 predicted values results more coherent with the real values for a middle range of
1689 B_d values. In particular we identified a range that goes between 0.8 to 1.6 g cm⁻³,
1690 which falls within the typical range of B_d found in Irish grassland soils, where
1691 the model returns B_d values close to real values. In these cases the model is
1692 more robust, predicting a numerical estimate with a quite low standard error.
1693 Furthermore, neither overestimation nor underestimation prevails for a middle
1694 range of B_d .
1695
1696
1697
1698
1699
1700
1701

1702 The model shows the higher errors for the extreme B_d classes, namely (i) very
1703 low B_d , that we identified as values lower than 0.8 g cm⁻³, or (ii) very high B_d
1704 values, identified as values higher than 1.6 g cm⁻³. The algorithm appears to a
1705 have higher prediction power on medium B_d values which also receive higher
1706
1707
1708
1709
1710
1711

1712
1713
1714
1715
1716
1717
1718
1719
1720
1721
1722
1723
1724
1725
1726
1727
1728
1729
1730
1731
1732
1733
1734
1735
1736
1737
1738
1739
1740
1741
1742
1743
1744
1745
1746
1747
1748
1749
1750
1751
1752
1753
1754
1755
1756
1757
1758
1759
1760
1761
1762
1763
1764
1765
1766
1767
1768
1769
1770

representation in our dataset. In general, machine learning algorithms are improved where greater input data is provided. Therefore, in our case, the algorithm is inherently biased towards the correct prediction of medium ranges.

3.3 Models choice considerations

We have chosen to use decision trees and linear regression because these simple types of models allow users to identify the B_d class (for decision trees), and the B_d value (for linear regression) without the need to rely on additional software. Furthermore, besides the predictive ability, decision trees also provide descriptive power, in that they make explicit the relationships among different characteristics of the soils and allow the user to have greater insight to these relationships. Other algorithms that were considered, i.e., support vector machines and multi-layer perceptron, although leading to similar performance, do not allow this type of insight. A full comparison between different algorithms, from the performance point of view, can be conducted in future. While the quality of the interrogated database was good, we believe that further improvement of model performance can be achieved by increasing the extent of the sample dataset, especially for horizons with low and high B_d values, which are less represented in our data. Finally, the utility of these models to assess critical thresholds for compaction should be evaluated for descriptive soil datasets where attributes such as “Compact degree” (FAO, 2006) are included.

4. Conclusion

A decision tree and linear equation model were developed to predict soil bulk density on the basis of visual descriptors. The visual soil descriptors identified, as being more informative by both models, are associated with specific soil properties. This allows the user to rank to these properties in terms of their impact on soil structural quality. For both models the most relevant properties

1771
1772
1773 that affect B_d appears to be soil humic characteristics, followed by soil porosity
1774 and pedogenic formation.
1775
1776

1777 Overall, the decision tree model shows an accuracy of about 60%, while the
1778 linear equation model had a correlation coefficient of about 0.65 with respect to
1779 the measured B_d values. The two models are parsimonious and can be used by
1780 soil surveyors and analysts who need to have a quick and approximate *in-situ*
1781 estimate of the structural quality for various soil functional applications.
1782 Furthermore they have an enormous potential to retrofit B_d data (i.e. gap fill) to
1783 existing data sets where laboratory data are missing. Future work is required to
1784 refine these models for use on soils with very low and very high B_d classes
1785 which fall outside those typically found in Ireland. Finally, our goal is to encode
1786 the decision tree and the linear equation into a mobile application, in order to
1787 enable multiple user types to perform B_d prediction more quickly, on site, and in
1788 a user friendly manner.
1789
1790
1791
1792
1793
1794
1795
1796
1797
1798
1799
1800

1801 **Acknowledgements**

1802

1803 The authors thank Irene Marongiu for her help with the physical and chemical
1804 soil analyses. SQUARE project has received funding from the Irish
1805 Department of Agriculture (DAFM) Research Stimulus Fund (RSF). Task 3
1806 output.
1807
1808
1809
1810

1811 **References**

1812

- 1813
1814 Alvarez, S.A., 2002. An exact analytical relation among recall, precision, and
1815 classification accuracy in information retrieval. Tech. Rep. BCCS-02-01,
1816 Computer Science Department, Boston College.
1817
1818
1819 Ampoorter, E., Goris, R., Cornelis, W. M., Verheyen, K., 2007. Impact of
1820 mechanized logging on compaction status of sandy forest soils. *Forest Ecol.*
1821 *Manag.* 241, 162–174.
1822
1823
1824 Armindo, R.A., Wendroth, O. 2016. Physical soil structure evaluation based on
1825 hydraulic energy functions. *Soil Sci. Am. J.* 80, 1167–1180.
1826
1827
1828
1829

- 1830
1831
1832
1833 Attou, F., Bruand, A., Bissonnais, Y. L., 1998. Effect of clay content and silt-
1834 clay fabric on stability of artificial aggregates. *Eur. J. Soil Sci.* 49, 569–577.
1835
- 1836 Ball, B. C., Munkholm, L. J., 2015. *Visual Soil Evaluation: Realizing Potential*
1837 *Crop Production with Minimum Environmental Impact.* CAB International.
1838 London.
1839
- 1840
1841 Batey, T., 2000. Soil profile description and evaluation. In: Smith, K., Mullins,
1842 C. (Eds.), *Soil and environmental analysis, physical methods*, 2nd edition.
1843 Marcel Dekker, New York. pp. 595–628
1844
- 1845
1846 Bhargava, N., Sharma, G., Bhargava, R., Mathuria, M., 2013. Decision tree
1847 analysis on j48 algorithm for data mining. *Proceedings of International*
1848 *Journal of Advanced Research in Computer Science and Software*
1849 *Engineering.* 3, 1114–1119.
1850
- 1851
1852 Boix-Fayos, C., Calvo-Cases, A., Imeson, A.C., 2001. Influence of soil
1853 properties on the aggregation of some Mediterranean soils and the use of
1854 aggregate size and stability as land degradation indicators. *Catena* 44, 47–67.
1855
- 1856
1857 Bronick, C. J., Lal, R. 2005. Soil structure and management: a review.
1858 *Geoderma.* 124, 3–22.
1859
- 1860
1861 Caravaca, F., Hernandez, T., Garcia, C., Roldan, A., 2002. Improvement of
1862 rhizosphere aggregate stability of afforested semiarid plant species subjected
1863 to mycorrhizal inoculation and compost addition. *Geoderma.* 108, 133–144.
1864
- 1865
1866 Collins, J. F., Larney, F. J., Morgan, M. A., 2004. Climate and soil
1867 management, in: Keane, T., Collins, J. F. (Eds.), *Climate, Weather and Irish*
1868 *Agriculture. Working group on Applied Agricultural Meteorology*
1869 *(AGMET), Dublin*, pp. 119–160.
1870
- 1871
1872 Creamer, R., Simo, I., Reidy, Carvalho, J., Fealy, R., Hallett, S., Jones, R.,
1873 Holden, A., Holden, N., Hannam, J., Massey, P., Mayr, T., McDonald, E.,
1874 O'Rourke, S., Sills, P., Truckell, I., Zawadzka, J., Schulte, R., 2014. *Irish*
1875 *Soil Information System. (2007-S-CD-1-S1) EPA STRIVE Programme*
1876 *2007–2013, Synthesis Report.*
1877
- 1878
1879
1880
1881 Dam, R.F., Mehdi, B.B., Burgess, M.S.E., Madramootoo, C.A., Mehuys, G.R.,
1882 Callum, I.R., 2005. Soil bulk density and crop yield under eleven
1883
1884
1885
1886
1887
1888

1889
1890
1891
1892 consecutive years of corn with different tillage and residue practices in a
1893 sandy loam soil in central Canada. *Soil Till. Res.* 84, 41–53.
1894

1895 Deconchat, M., 2001. Effets des techniques d'exploitation forestie`res sur
1896 l'e'tatde surface du sol. *Ann. For. Sci.* 58, 653–661.
1897

1898
1899 Dexter, A. R., 1988. Advances in characterization of soil structure, *Soil Till.*
1900 *Res.* 11, 199–238.
1901

1902 Dexter, A. R., 2002. Soil structure: the key to soil function, in: Pagliai, M.,
1903 Jones, R., (Eds.), *Sustainable land Management – Environmental Protection,*
1904 *a soil Physical Approach.* *Advances in Geocology* 35, Clearance Center,
1905 Inc., Reiskirchen, pp. 57–69.
1906
1907

1908
1909 Ellert, B. H., Bettany, J. R., 1995. Calculation of organic matter and nutrient
1910 stored in soils under constrain management regimes. *Can. J. Soil Sci.* 75,
1911 529–538.
1912

1913
1914 Emmet-Booth, J. P., Forristal, P. D., Fenton, O., Ball, B. C., Holden, N. M.,
1915 2016. A review of visual soil evaluation techniques for soil structure. *Soil*
1916 *Use Manage.* 32, 623–634.
1917

1918
1919 Epron, D., Plain, C., Ndiaye, F. K., Bonnaud, P., Pasquier, C., Ranger, J., 2016.
1920 Effects of compaction by heavy machine traffic on soil fluxes of methane
1921 and carbon dioxide in a temperate broadleaved forest. *Forest Ecol. Manag.*
1922 382, 1–9.
1923
1924

1925
1926 FAO, 2006. *Guidelines for Soil Description, Fourth Edition.* FAO, Rome.

1927
1928 FAO, ISRIC, ISSS, 1998. *World Reference Base for Soil Resources.* *World Soil*
1929 *Resources Reports* 80, FAO Rome.
1930

1931 Fenton, O., Vero, S., Ibrahim, T. G., Murphy, P. N. C., Sherriff, S. C.,
1932 ÓHuallacháin, D., 2015. Consequences of using different soil texture
1933 determination methodologies for soil physical quality and unsaturated zone
1934 time lag estimates. *J Contam. Hydrol.* 182, 16–24.
1935
1936

1937
1938 Fenton, O., Vero, S., Schulte, R.P.O., O'Sullivan, L., Bondi, G., Creamer, R.E.,
1939 2017. Application of Dexter's soil physical quality index: an Irish case study
1940 *Irish J. Agr. Food.* 56, 45–53.
1941
1942
1943
1944
1945
1946
1947

- 1948
1949
1950
1951 Geissen, V., Kampichler, C., López-de Llergo-Juárez, J. J., Galindo-Acántara,
1952 A., 2007. Superficial and subterranean soil erosion in Tabasco, tropical
1953 Mexico: development of a decision tree modeling approach. *Geoderma*. 139,
1954 277–287.
1955
1956
1957 Håkansson, I., Lipiec, J., 2000. A review of the usefulness of relative bulk
1958 density values in studies of soil structure and compaction. *Soil Till. Res.* 53,
1959 71–85.
1960
1961
1962 Haynes, R.J., Naidu, R., 1998. Influence of lime, fertilizer and manure
1963 applications on soil organic matter content and soil physical conditions: a
1964 review. *Nutr. Cycl. Agroecosyst.* 51, 123–137.
1965
1966
1967 Henderson, B. L., Bui, E. N., Moran, C. J., Simon, D. A. P., 2005. Australia-
1968 wide predictions of soil properties using decision trees. *Geoderma*. 124, 383–
1969 398.
1970
1971
1972 Holden, N., Brereton, A.J., 2004. Definition of agroclimatic regions in Ireland
1973 using hydro-thermal and crop yield data. *Agr. Forest Meteorol.* 122, 175–
1974 191.
1975
1976
1977 IUSS Working Group WRB, 2006. World Reference Base for Soil Resources –
1978 a framework for international classification, correlation and communication.
1979 World Soil Resources Reports 103. FAO, Rome.
1980
1981
1982 Jin, R., Li, X., Che, T., 2009. A decision tree algorithm for surface soil
1983 freeze/thaw classification over China using SSM/I brightness temperature.
1984 *Remote Sens. Environ.* 113, 2651–2660.
1985
1986
1987 Karlen, D.L., 2004. Soil quality as an indicator of sustainable tillage practices.
1988 *Soil Till. Res.* 78, 129–130.
1989
1990
1991 Kaur, R., Sanjeev, K., Gurung, H., 2002. Apedo-transfer function (PTF) for
1992 estimating soil bulk density from basic soil data and its comparison with
1993 existing PTFs. *Aust. J. Soil Res.* 40, 847–857.
1994
1995
1996 Kay, B.D., 1998. Soil structure and organic carbon: a review. In: Lal, R.,
1997 Kimble, J.M., Follett, R.F., Stewart, B.A. (Eds.), *Soil Processes and the*
1998 *Carbon Cycle*. CRC Press, Boca Raton, pp. 169-197.
1999
2000
2001 Kay, B.D., Hajabbasi, M.A., Ying, J., Tollenaar, M., 2006. Optimum versus
2002 non-limiting water contents for root growth, biomass accumulation, gas
2003
2004
2005
2006

- 2007
2008
2009
2010
2011
2012
2013
2014
2015
2016
2017
2018
2019
2020
2021
2022
2023
2024
2025
2026
2027
2028
2029
2030
2031
2032
2033
2034
2035
2036
2037
2038
2039
2040
2041
2042
2043
2044
2045
2046
2047
2048
2049
2050
2051
2052
2053
2054
2055
2056
2057
2058
2059
2060
2061
2062
2063
2064
2065
- exchange and the rate of development of maize (*Zea mays* L.). *Soil Till. Res.* 88, 42–54.
- Lee, K. E., Foster, R. C., 1991. Soil fauna and soil structure. *Aust. J. Soil Res.* 29, 745–775.
- Leonavičiutė, N., 2000. Predicting soil bulk and particle densities by pedotransfer functions from existing soil data in Lithuania, *Geografijos metraštis*. 33, 317–330.
- Logsdon, S.D., Karlen, D.L., 2004. Bulk density as a soil quality indicator during conversion to no-tillage. *Soil Till. Res.* 78, 143–149.
- Moncada, M.P., Ball, B.C., Gabriels, D., Lobo, D. and Cornelis, W.M., 2015. Evaluation of soil physical quality index S for some tropical and temperate medium-textured soils. *Soil Sci. Soc. America J.* 79, 9–19
- Mueller, L., Kay, B. D., Deen, B., Hu, C., Zhang, Y., Wolff, M., Eulenstein, F., Schindler, U., 2009. Visual assessment of soil structure: Part II. Implications of tillage, rotation and traffic on sites in Canada, China and Germany. *Soil Till. Res.* 103, 188–196.
- Pachepsky, Y. A., Rawls, W. J., 2003. Soil structure and pedotransfer functions. *Eur. J. Soil Sci.* 54, 443–452.
- Pagliai, M., Vignozzi, N., 2002. The soil pore system as an indicator of soil quality, in: Pagliai, M., Jones, R., (Eds.), *Sustainable land Management – Environmental Protection, a soil Physical Approach*. *Advances in Geocology* 35, Clearance Center, Inc., Reiskirchen, pp. 71–82.
- Quinlan, J. R., 1993. *C4.5: Programs for Machine Learning*. Morgan Kaufmann Publishers.
- Reidy, B., Simo, I., Sills, P., Creamer, R. E., 2016. Pedotransfer functions for Irish soils-estimation of bulk density (ρ_b) per horizon type. *Soil*. 2, 25–39.
- Russell, E. W., 1975. *Soil Conditions and Plant Growth* 10th edition. Ed. Longman, London.
- Saffih-Hdadi, K., Défossez, P., Richard, G., Cui, Y. J., Tang, A. M., Chaplain, V., 2009. A method for predicting soil susceptibility to the compaction of

2066
2067
2068 surface layers as a function of water content and bulk density, *Soil Till. Res.*
2069 105, 96–103.
2070
2071

2072 Schoeneberger, P.J., D.A. Wysocki, E.C. Benham, and Soil Survey Staff. 2012.
2073 Field book for describing and sampling soils, Version 3.0. Natural Resources
2074 Conservation Service, National Soil Survey Center, Lincoln, NE.
2075
2076

2077 Schulten, H.R., Leinweber, P., 2000. New insights into organic– mineral
2078 particles: composition, properties and models of molecular structure. *Biol.*
2079 *Fertil. Soils.* 30, 399– 432.
2080
2081

2082 Shipitalo, M. J., Le Bayon, R. C., 2004. 10 Quantifying the Effects of
2083 Earthworms on Soil Aggregation and Porosity, in: Edwards, C.A. (Eds.)
2084 Earthworm ecology 2nd edition, Boca Raton, pp 183–199.
2085
2086

2087 Soil Survey Division Staff, 1993. Soil Survey Manual. Agricultural Handbook
2088 N 18. USDA Natural Resources Conservation Service, Washington D.C.
2089
2090

2091 Stevenson, F.J. 1994. Humus chemistry. genesis, composition, reactions. 2nd
2092 edition. Wiley Interscience, New York.
2093
2094

2095 Teepe, R., Brumme, R., Beese, F., Ludig, B., 2004. Nitrous oxide emission and
2096 methane consumption following compaction of forest soils. *Soil Sci. Soc.*
2097 *Am. J.* 68, 605–611.
2098
2099

2100 Templ, M., Kowarik, A., & Filzmoser, P., 2011. Iterative stepwise regression
2101 imputation using standard and robust methods. *Comput. Stat. Data An.* 55,
2102 2793–2806.
2103
2104

2105 Xue, D., De Baets, B., Van Cleemput, O., Hennessy, C., Berglund, M., Boeckx,
2106 P., 2013. Classification of nitrate polluting activities through clustering of
2107 isotope mixing model outputs. *J. Environ. Qual.* 42, 1486–1497.
2108
2109

2110 Xue, D., Pang, F., Meng, F., Wang, Z., Wu, W., 2015. Decision-tree-model
2111 identification of nitrate pollution activities in groundwater: A combination of
2112 a dual isotope approach and chemical ions. *J. Contam. Hydrol.* 180, 25–33.
2113
2114
2115
2116
2117
2118
2119
2120
2121
2122
2123
2124

Table 1. Selection of soil structure field descriptors described by FAO, Guidelines for Soil Description, 2006.

Descriptor	Title	Description
1	Humose	This is an estimation of the degree of humification of the organic material. Surveyor must provide a positive or affirmative answer to being humose (this descriptor was recorded as a presence/absence in the database).
2	Soil Consistency	The strength with which soil materials are held together. It provides a means of describing the degree of cohesion and adhesion between the soil particles as related to the resistance of the soil to deform or rupture. It includes soil properties such as friability, plasticity, stickiness and resistance to compression. It changes with soil moisture and is highly related to the percentage of clay and OM in the soil.
3	Stickiness	It is the capacity of the soil to adhere to an object. It is evaluated pressing a small amount of wet soil between thumb and forefinger to see if it will stick to fingers.
4	Plasticity	The ability of soil material to retain a shape after pressure deformation. It is evaluated by rolling a small amount of wet soil between the hand palms until it forms a long, round strip like a wire about 3 mm thick.
Soil structure* is described as the combination of (5, 6, 7)		
5	Structure Grade	It describes the level of development of soil structure. It is expressed as the differential between cohesion within aggregates and adhesion between aggregates. It is evaluated in relation to the arrangement of the aggregates and to the strength necessary to break them.
6	Structure Type	It describes the form or shape of individual aggregates and is directly correlated with the pedogenic formation.
7	Structure Size	It describes the average size of individual aggregates. Different classes may be recognized in relation to the type of soil structure from which they come.
Voids** is described as the combination of (8, 9)		
8	Voids Abundance	An indication of the total volume of voids measured by area and was recorded as the percentage of the surface occupied by pores.
9	Voids Size	The diameter of voids and was recorded in mm.
10	Fissures size	The diameter of fissures and was recorded in mm.
11	Macropores size	The diameter of macropores, which are described as bigger void, mostly determined by plant roots, and by zoological exploration. Macropores were recorded in mm.
*Soil Structure: It refers to the spatial disposition of aggregates which are the result of the aggregation of single particles such as sand, silt and clay. Size, shape and arrangement of these solids and voids, determining the porosity and the capacity to retain fluids and inorganic and organic substances can occur in different patterns, resulting in different soil structures (Bronick et Lal, 2005).** Voids: Include all the pore space present in the soil. It is closely related to the porosity and is a good indicator of soil compactness. It is evaluated as presence/absence data. Voids were described in terms of size and abundance.		

Table 2. Decision tree model (Model 1); performances. RMSE: Root Mean Squared Error; MAE: Mean Absolute Error

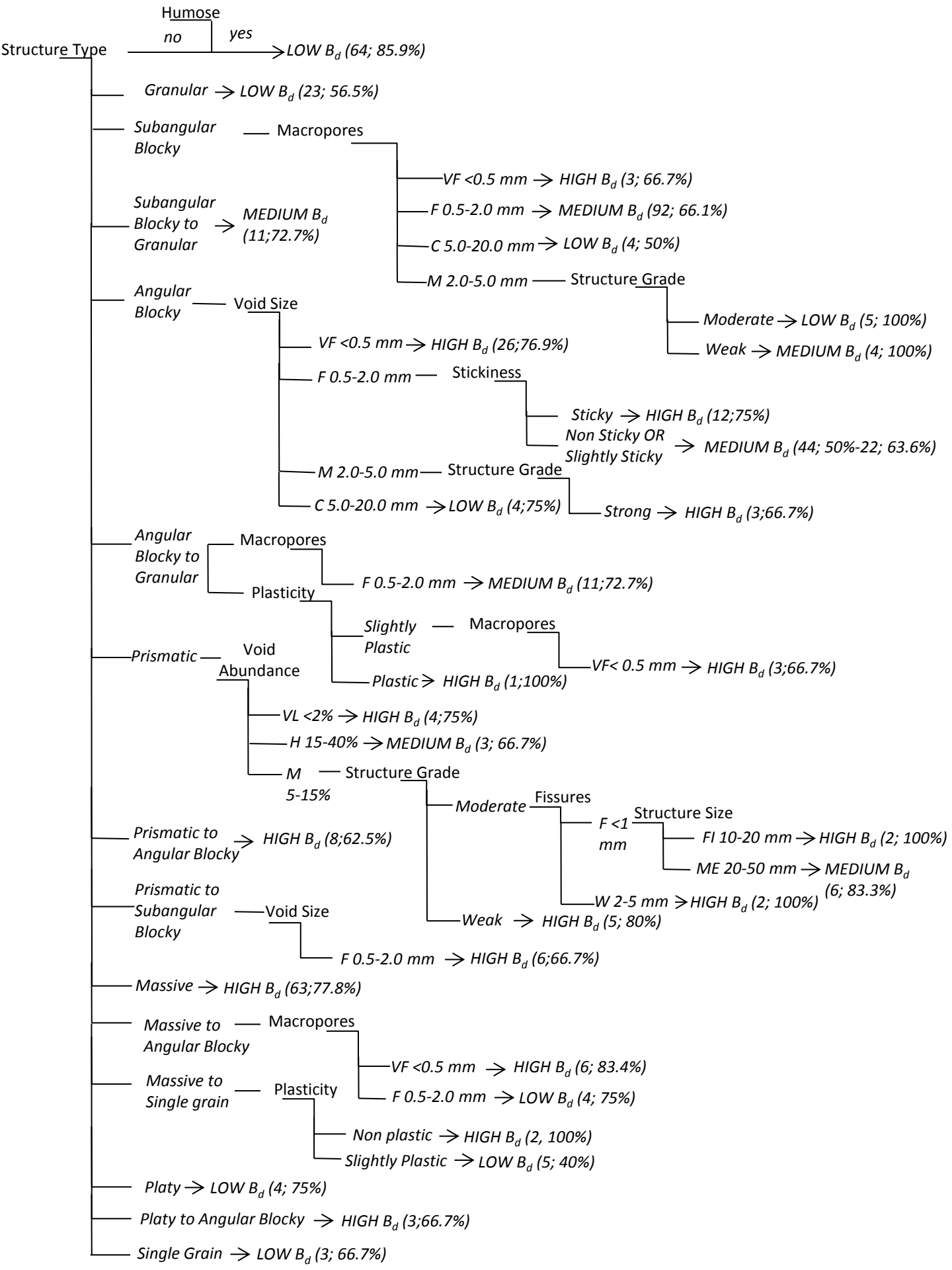
	Performance with cross validation				Performance on training set			
	N. of instances	Accuracy	RMSE	MAE	N. of instances	Accuracy	RMSE	MAE
Correctly Classified Instances	283	60.08 %	0.44	0.32	335	71.12%	0.37	0.27
Incorrectly Classified Instances	188	39.91 %			136	28.87 %		
	N. of instances	Precision	Recall	F-measure	N. of instances	Precision	Recall	F-measure
Low B_d class	137	0.70	0.54	0.60	137	0.75	0.65	0.69
Medium B_d class	178	0.53	0.63	0.58	178	0.64	0.73	0.68
High B_d class	156	0.62	0.62	0.62	156	0.76	0.74	0.75
Weighted Average		0.61	0.60	0.60		0.72	0.71	0.71

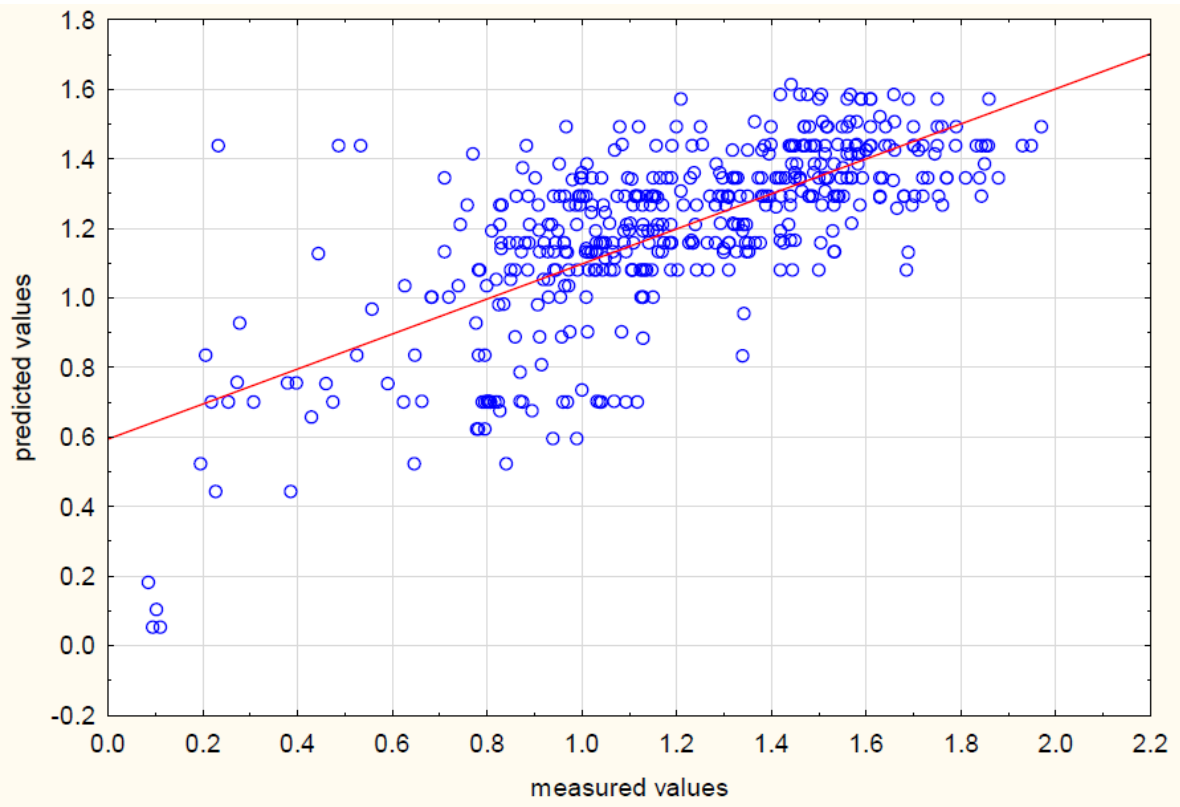
Table 3. Decision tree model (Model 1); confusion matrix.

Classes classified by decision tree model (N. of instances=471)			
	a	b	c
Low B_d class (a)	74	46	17
Medium B_d class (b)	25	112	41
High B_d class (c)	7	52	97

Table 4. Linear regression model (Model 2); performances. RMSE: Root Mean Squared Error; MAE: Mean Absolute Error

	Performance with cross validation				Performance on training set			
	N. of instances	Correlation coefficient	RMSE	MAE	N. of instances	Correlation coefficient	RMSE	MAE
Instances	471	0.65	0.27	0.21	471	0.71	0.25	0.20





Figures Captions:

Figure 1. Decision tree model for predicting bulk density classes (Model 1): LOW $B_d < 1 \text{ g cm}^{-3}$; MEDIUM $B_d 1-1.4 \text{ g cm}^{-3}$; HIGH $B_d > 1.4 \text{ g cm}^{-3}$. The number of cases classified for the rule and the percentage of accuracy are reported.

Figure 2. Decision tree model for predicting bulk density classes (Model 1): MEDIUM $B_d 1-1.4 \text{ g cm}^{-3}$. The number of cases classified for the rule and the percentage of accuracy are reported.

Figure 3. Decision tree model for predicting bulk density classes (Model 1): HIGH $B_d > 1.4 \text{ g cm}^{-3}$. The number of cases classified for the rule and the percentage of accuracy are reported.

Figure 42. Relationship between measured bulk density (B_d) and predicted bulk density values for the linear regression model (Model 2). B_d values are reported in g cm^{-3} .

Figures Captions:

Figure 1. Decision tree model for predicting bulk density classes (Model 1): LOW $B_d < 1 \text{ g cm}^{-3}$; MEDIUM $B_d 1-1.4 \text{ g cm}^{-3}$; HIGH $B_d > 1.4 \text{ g cm}^{-3}$. The number of cases classified for the rule and the percentage of accuracy are reported.

Figure 2. Relationship between measured bulk density (B_d) and predicted bulk density values for the linear regression model (Model 2). B_d values are reported in g cm^{-3} .

Supplementary Material Table 1. Field descriptors choice options. Abbreviation and definitions.

Field Descriptor	Full Name	Abbreviation/Definition
1. Humose		
	No Humic	NH
	Humic	H
2. Soil Consistency		
	Loose	LO: Non-coherent.
	Very friable	VFR: Crushes under very gentle pressure, but coheres when pressed together.
	Friable	FR: Crushes under gentle to moderate pressure between thumb and forefinger and coheres when pressed together.
	Firm	FI: Crushes under moderate pressure between thumb and forefinger; resistance is noticeable.
	Very firm	VFI: Crushes under strong pressure; barely crushable between thumb and forefinger.
3. Stickiness		
	Extremely firm	EFI: Crushes under only very strong pressure; cannot be crushed between thumb and forefinger.
	Non-sticky	NST: No soil material adheres to thumb and finger after release of pressure.
	Slightly sticky	SST: Soil material adheres to thumb and finger after release of pressure, but it is easily removed.
	Sticky	ST: Soil material adheres to thumb and finger after release of pressure, and tends to stretch and pull apart rather than coming away from each digit.
	Very sticky	VST: Soil material adheres strongly to thumb and finger after release of pressure, and stretches when fingers are separated.
4. Plasticity		
	Non-plastic	NPL: No wire is formable.
	Slightly plastic	SPL: Wire formable but breaks immediately if bent into a ring; deformation by slight force.
	Plastic	PL: Wire formable but breaks if bent into a ring; deformation by slight to moderate force.
	Very plastic	VPL: Wire formable and can be bent into a ring; deformation by moderately strong to strong force.
5. Structure Grade		
	Weak	WE; Aggregates barely visible in situ and only weak arrangement of natural surfaces that breaks when gently disturbed.
	Moderate	MO: Aggregates are visible in situ and there is a distinct arrangement of material. When disturbed it breaks into a mixture of entire and broken aggregates.
	Strong	ST: Aggregates are clearly visible in situ and there is prominent arrangement of material. When disturbed it breaks into distinct whole aggregates.

	Weak to Moderate	WM: Show weak and moderate properties
	Moderate to strong	MS: show moderate and strong properties.
6. Structure Type		
	Granular	GR
	Granular to Single Grain	GRSG
	Angular Blocky	AB
	Angular Blocky to Granular	ABGR
	Subangular Blocky	SB
	Subangular Blocky to Granular	SBGR
	Prismatic	PR
	Prismatic to Angular Blocky	PRAB
	Prismatic to Subangular Blocky	PRSB
	Platy	PL
	Platy to Angular Blocky	PLAB
	Platy to Subangular Blocky	PLSB
	Single Grain	SG
	Massive	MA
	Massive to Single Grain	MASG
Massive to Angular Blocky	MAAB	
7. Structure Size*	*Structure size is evaluated taking into account the main categories of structure type in the following order.	
Blocky	Coarse	C : 20-50mm
Prismatic/Columnar	Coarse	C : 50-100mm
Granular/Platy	Coarse	C : 5-10mm
Prismatic/Columnar	Fine	F : 10-20mm

Granular/Platy	Fine	F : 1-2mm
Blocky	Fine	F : 5-10mm
Blocky	Medium	M : 10-20mm
Prismatic/Columnar	Medium	M : 20-50mm
Granular/Platy	Medium	M : 2-5mm
Prismatic/Columnar	Very Coarse	VC : > 100mm
Granular/Platy	Very Coarse	VC: > 10mm
Blocky	Very Coarse	VC: > 50mm
Prismatic/Columnar	Very Fine	VF: < 10mm
Granular/Platy	Very Fine	VF: < 1mm
Blocky	Very Fine	VF: < 5mm
8. Voids Abundance		
	Very Low	VL: <2%
	Low	L: 2-5%
	Medium	M: 5-15%
	High	H: 15-40%
	Very High	VH: >40%
9. Voids Size		
	Very Fine	VF: < 0.5mm
	Fine	F: 0.5-2 mm
	Medium	M: 2-5 mm
	Coarse	C : 5-20 mm
	Very Coarse	VC: 20-50mm
10. Fissures Size		
	Fine	F: < 1mm
	Medium	M: 1-2 mm
	Wide	W: 2-5 mm

	Very Wide	VW: 5-10 mm
	Extremely Wide	EW: > 10mm
11. Macropores Size		
	Very Fine	VF: < 0.5mm
	Fine	F : 0.5-2 mm
	Medium	M : 2-5 mm
	Coarse	C : 5-20 mm
	Very Coarse	VC : 20-50mm

Supplementary Material Table 2. Total list of rules for Model 1.

Rule n.	Bulk density Class	Description
1	Low	Humose=Yes
2	Low	Humose=No AND Structure type=Granular
3	Low	Humose=No AND Structure type=Subangular Blocky AND Macropores= M 2.0-5.0 mm AND Structure Grade=Moderate
4	Low	Humose=No AND Structure type=Subangular Blocky AND Macropores= C 5.0-20 mm
5	Low	Humose=No AND Structure type=Angular Blocky AND Void Size= C 5.0-20 mm
6	Low	Humose=No AND Structure type=Angular Blocky AND Void Size= F 0.5-2.0 mm AND Stickiness= Very Sticky
7	Low	Humose=No AND Structure type=Single Grain
8	Low	Humose=No AND Structure type=Massive to Angular Blocky AND Macropores= F 0.5-2.0 mm
9	Low	Humose=No AND Structure type=Prismatic to Subangular Blocky AND Void Size= M 2.0-5.0 mm
10	Low	Humose=No AND Structure type=Platy
11	Low	Humose=No AND Structure type=Massive to Single grain AND Plasticity= Slightly Plastic
12	Medium	Humose=No AND Structure type=Subangular Blocky AND Macropores F 0.5-2 mm
13	Medium	Humose=No AND Structure type=Subangular Blocky AND Macropores M 2.0-5.0 mm AND Structure Grade= Weak
14	Medium	Humose=No AND Structure type=Angular Blocky AND Void size= M 2-5 mm AND Structure Grade= Moderate
15	Medium	Humose=No AND Structure type=Angular Blocky AND Void size= F 0.5-2 mm AND Stickiness= Non Sticky
16	Medium	Humose=No AND Structure type=Angular Blocky AND Void size= F 0.5-2 mm AND Stickiness= Slightly Sticky
17	Medium	Humose=No AND Structure type=Prismatic AND Void abundance= H 15-40%
18	Medium	Humose=No AND Structure type=Prismatic AND Void abundance= M 5-15% AND Structure Grade= Moderate AND Fissures= F <1 mm AND Structure Size= ME 20-50 mm
19	Medium	Humose=No AND Structure type=Prismatic AND Void abundance= M 5-15% AND Structure Grade= Moderate AND Fissures= F <1 mm AND Structure Size= CO 50-100 mm
20	Medium	Humose=No AND Structure type=Prismatic AND Void abundance= M 5-15% AND Structure Grade= Strong

21	Medium	Humose=No AND Structure type=Prismatic to Subangular Blocky AND void size=VF <0.5 mm
22	Medium	Humose=No AND Structure type= Subangular Blocky to Granular
23	Medium	Humose=No AND Structure type= Angular Blocky to Granular AND Macropores= F 0.5-2.0 mm
24	Medium	Humose=No AND Structure type= Angular Blocky to Granular AND Macropores= M 2.0-5.0 mm
25	High	Humose=No AND Structure type= Massive
26	High	Humose=No AND Structure type= Subangular Blocky AND Macropores= VF <0.5 mm
27	High	Humose=No AND Structure type= Angular Blocky AND Void size= M 2.0-5.0 mm AND Structure grade= Strong
28	High	Humose= No AND Structure type= Angular blocky AND Void size=F 0.5-2 mm AND Stickiness= Sticky
29	High	Humose=No AND Structure type= Angular blocky AND Void size= VF <0.5 mm
30	High	Humose=No AND Structure type= Prismatic AND Void abundance= M 5-15% AND Structure grade= Moderate AND Fissures= F <1mm AND Structure size= FI 10-20 mm
31	High	Humose=No AND Structure type= Prismatic AND Void abundance= M 5-15% AND Structure grade= Moderate AND Fissures= W 2.0-5.0 mm
32	High	Humose=No AND Structure type= Prismatic AND Void abundance= M 5-15% AND Structure grade= Weak
33	High	Humose=No AND Structure type= Prismatic AND Void Abundance=VL
34	High	Humose=No AND Structure type= Prismatic to Angular Blocky
35	High	Humose= No AND Structure type= massive to Angular Blocky AND Macropores=VF < 0.5 mm
36	High	Humose=No AND Structure type= Prismatic to Subangular Blocky AND Void size= F 0.5-2 mm
37	High	Humose=No AND Structure type= Platy to Angular Blocky
38	High	Humose=No AND Structure type=Massive to Single grain AND Plasticity= Non Plastic
39	High	Humose=No AND Structure Type=Angular Blocky to Granular AND Plasticity=Slightly plastic AND Macropores= VF< 0.5 mm
40	High	Humose=No AND Structure type= Angular Blocky to Granular AND Plasticity=Non plastic
41	High	Humose=No AND Structure type= Angular Blocky to Granular AND Plasticity= Plastic